Politecnico di Torino · Facoltà di Ingegneria

Tool development for preliminary design of next generation low pressure turbines

Tesi di Laurea Magistrale

Corso di Laurea in Ingegneria Aerospaziale

Tutor:
Prof. Daniele Botto
Ing. Paride Mesaglio Chittaro

Candidate:
Domenico Piccirillo

Marzo 2019

Summary

The purpose of this thesis work concerns the development of a tool named PRIME, able to provide quick and easy aeromechanical feedback in the preliminary design of a low pressure turbine of aeronautical engines. This tool presents a considerable improvement in the preliminary design loops, thereby making the project process more robust and smart both on aerodynamic and aeromechanical side. The benefits are related to a reduction of misunderstanding and data exchange error beyond time and resources savings.

The tool workflow begins with the 3D CAD airfoil creation, starting from geometry finalization handles in the Unigraphics NX environment, and considering parametric templates which represent mechanical arrangements on low pressure turbine stage outside the main flow paths. The second step of automatic design system is to generate the FEM model (developed in ANSYS Workbench environment) of above mentioned turbine stages with customizable boundary conditions to run static and modal analysis according to internal design practice.

The contribution to this work focuses on CAD part to extend the capabilities of the exiting, in house developed tool (named DynBooster), for the cad generation. The whole code has been modified substantially so as to make it more lightweight and flexible. Furthermore, several parametric templates were generated, starting from creation of the cross-section sketch with a simple and robust logic in order to achieve more realistic results. On completion of this part, a new GUI allows the user to choose any template and modify all the parameters that define its geometry. In this way the user can create about 96 configurations so as to test new innovative LPT geometry. In addition, for the transition between imperial and metric units, a converter tool has been inserted.

Eventually, the tool has been integrated with wizard (the current process FEM generation build in ANSYS Workbench) and tested, launching static analysis with subsequent generation of Campbell diagrams.

In the future development of this tool it is foreseen to add a producibility package. This plug-in would introduce the possibility to realize a CAD model which takes into account the manufacturing process capability and thus makes synergy between component design and production.

Contents

List of Figures

Chapter 1

Introduction

1.1 The G2020 Project

This thesis takes place in an important aeronautical project called GREAT 2020 (Green Engine for Air Traffic 2020). This project was born in 2009, sets its main goals in efficiency and eco-friendliness, as requested by the European commission and the group of experts ACARE (Advisory for Aviation Research and Innovation in Europe).

Basically, the main aims are to reach a reduction of CO_2 emissions by 20%, a drastic reduction of NOx emissions by 80% and to reduce acoustic noise of 10dB in proximity to the ground. The future of the aeronautical sector is to make available more efficient engine that will not only burn less fuel but will also reduce damaging emissions, and to achieve this, it is necessary to put in place a new concept engine that will incorporate new aerodynamic design, material, combustion and cooling technology. [1] These are the guidelines of this thesis which mainly focuses on the development and implementation of a software dedicated to the aeromechanical analysis of low pressure turbine stages.

Great 2020 is the main challenge for all excellence sectors of the aeronautical industry with a synergic collaboration between industry and university. In particular play a key role:

- Avio Aero (GE Aviation Business) international industry in the manufacture, design and maintenance of aeronautical component. During more than a century it has reached technologic and manufacture leadership worldwide, thanks to continue investment in research and development and to ongoing collaboration with university.

- Politecnico di Torino one of the most important technical institutions. The departments of mechanics and aerospace engineering, applied science and technology, energy, management engineering and production take part in the GREAT 2020 project. Of particular relevance is the virtuous partnership with

Avio Aero that led to the creation of joint laboratory (Great Lab) located inside the polytechnic campus. The purpose of this lab is to coordinate sheared research activities, monitoring the international scientific landscape in order to identify innovative ideas and create a sector of integrated skills and human resources.

- ISTEC-CNR, a unit of institute of science and technology in Turin handles research in the ceramic material field, especially focused on the new environmentally friendly processes for the alloys of aeronautical interest in the Great 2020.

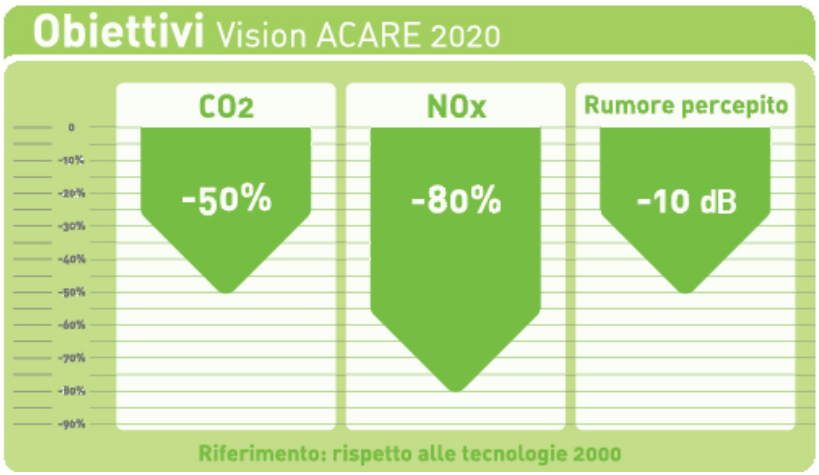

Figure 1.1: ACARE 2020 - main goals

The project has led to the creation of six specialized laboratories, composed by Avio Aero workers, institution researchers and enterprises in Piedmont. Each one of this laboratories has specific goals as Lift-Lab, that handles research new low density and high resistant material; Aeronflux-Lab, aiming to further maximizing of low pressure turbine efficiency; Ageades-Lab, that plans a robust system of mechanical transmission; Zec-Lab, that realize a new generation of combustion system following eco-friendly guidelines; Mc-Lab, manages to integrate a new health engine monitoring system of control and Ecopro-Lab, involved in consolidating the engineering techniques used in transformation and control processes of aeronautical components.

This project rises in the Piemontese aerospace district aiming to develop innovative technologies for new aeronautical engine generation and boasts the financial support by Piemonte region thanks to the European regional development fund. Also, a network of small and medium sized businesses in aerospace located in Piedmont territory take part in this challenge.

1.2 Thesis Purpose

This thesis takes part into a wider and innovative project which concerns the development of a tool (PRIME) used to carry out the preliminary design on LPT (low pressure turbine stage). This tool acts as a binding force between two important team cooperating a preliminary analysis, the aerodynamic and aeromechanics team, by introducing a new simulation method (Aero-Mech). An important point is to understand which the current process is followed by the company and the improvements that PRIME can bring of its use.

Usually the process begins in aerodynamic team with an in-depth study of aerodynamic design optimization and only then, when the result is optimal about energy exchanging the aeromechanical team comes in. In this new phase detail aeromechanical analyses carried out in order to have more-efficient and reliable high-performance machines for example shall be verified that blade vibration will be damped in the operating range. But not always the aerodynamic optimum satisfies mechanical and aeromechanical criteria, thus, an aerodynamics design optimization could lead to considerable time delay. The PRIME tool has been designed to fill the gap between aerodynamic and aeromechanic analysis, reducing the data exchange error and giving an immediate feedback about the process followed. This means time and resources savings.

This tool may be seen as a set of black-boxes bathed in a kind of glue called gateway that manages all the input and output of internal processes. The tool provides two working modes, optimization mode that sets all the aerodynamic design and full aero-mech mode. The main difference is that with optimization mode the aerodynamic team can receive feedback about profile performance also in aeromechanical field, in order to know if it has to change the geometry profile; while with aero-mech mode the aeromechanical team have already received the aerodynamic input, because the aerodynamic part is just frozen, and will take place more detail analysis as peanuts, Campbell etc.

The workflow of PRIME consists in creation of a CAD with DynBooster, property software of Avio Aero, or the user can insert an appropriate prt file and only after importing it in Finite Element environment. The tool has a friendly and intuitive interface where the user can perform different analysis such as static and modal analysis. The release works with Unigraphics NX and ANSYS Workbench even if the whole Avio Aero legacy is based on MSC Nastran, which is why every analysis has been validated with a comparison of results between Nastran and Workbench. Finally, the results can be displayed by means of a Spotfire Dashboard.

The contribution made with follow thesis work, focuses mainly on CAD generation through the DynBooster Tool and on Campbell generation of new blade configuration with Nastran-Workbench validation. In particular on DynBooster side the whole code has been modified substantially so as to make it more flexible and robust, written for most in Matlab and the part concerning the interface with NX in

C++. Furthermore, different parametric templates have been generated according to the type, blade, vane or other configuration, with a simple and detailed logic in order to have more realistic results. Finally, it has been deployed a GUI where the user can choose the end templates and settle about 96 different configurations in order to test new innovative LPT geometries.

Chapter 2

Aircraft Engine

In literature propulsion means "Forward thrust, indeed this word is derived from two Latin words: *pro* meaning before or forwards and *pellere* meaning to drive. Propulsion system is defined as the set of components able to generate the propulsion force in order to change whatever current state of motion the body is in.

The main characteristic of propulsion system is that the thrust is determined considering the momentum increase of fluid propulsion, which takes place outside the engine (propeller), inside the engine but with an external fluid (jet engine), or inside the engine with a stowed-on board fluid (rocket engine) [2]. Different sources of energy are available to generate the thrust, for instance:

- chemical energy generated by the chemical reaction between fuel and oxidant (it is the most important source of energy for the aerospace propulsion).
- nuclear energy, this is one of the issues being studied for interplanetary missions even if its use has been demonstrated to remain dangerous the control.
- solar energy, this source of energy is exploited to produce electrical energy then used by electrical thrusters, however it is hardly ever used because huge surfaces area of solar panel are used to produce the power required.

The propulsion systems can be divided mainly in two categories: propeller propulsion, where the thrust is produced by the increase of air momentum through rotational speed of the propeller and jet propulsion, where at least part of the thrust is generated through mass expulsion carried on board. The propeller propulsion has been the first category of propulsion used in aviation and works by giving shaft power for then speed up the fluid propulsion thanks to propeller movement. In a first moment the piston engine has been employed, and many improvements have been done during the years such as switch from water cooling to air cooling in order to improve the weight engine. However, this engine was not suitable from power to

weight ratio point of views and the performance are reduced with increased of the altitude, thats why the turboprop engine has been introduced.

The end of propeller propulsion shall be certified from entry of air breathing engine, where the propulsion fluid mainly consists from air that flows inside the engine. It has allowed to overcome the limit of propeller propulsion and allows air speed upper to the speed of sound. These engines have become the mainly system propulsion in aeronautical field, and thanks to the keen commercial interest it could be developed a progressive technological improvement in order to have increasingly performed engine. Even if the rocket engine has been the first developed engine, it was found to be unsuitable for the civil aviation, since had high fuel consuming and control difficult. But this engine has been a great success in a space field being the only system propulsion able to generate thrust into the void.

2.1 Main Architecture in Service

Across age different systems of air breathing engine have been studied and only same of these have been implemented in the civil aviation, whereas for other, their use was limited to some military applications and experimental vehicle (this can include ramjet or scramjet engines). In the following part, a classification of engine architecture in service will be defined, and in particular turboprop, turboshaft, turbojet and turbofan will be described.

2.1.1 Turboprop

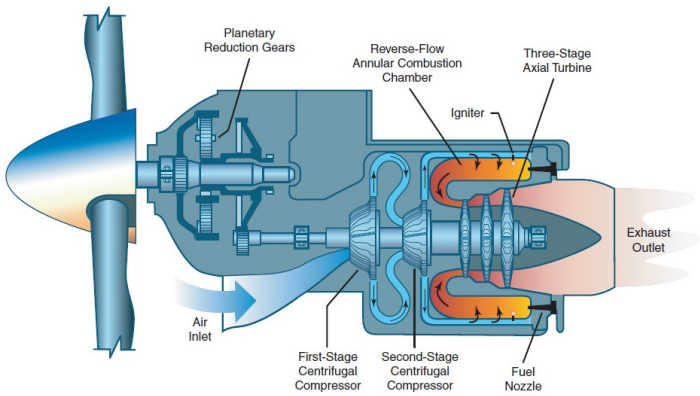

Figure 2.1: Turboprop architecturre[3]

The Turboprop engine was made in 1955 and is based on Brayton cycle. This engine introduces increased power to weight ratio and takes up a minimal amount

of frontal space, thereby ensuring lower aerodynamic resistance. As for the propeller engines, the turboprop uses internal combustion engine based on Brayton-Joule cycle and furthermore the compression and expansion are generated through rotating machines rather than alternative. Basically, the turboprop can be defined as mixed system, because part of thrust is generated by propeller and part is produced by jet. The dimension of propeller is much bigger compared to compressor and turbine, that is why the gearbox has to be introduced (in order to contain the rotational speed of the propeller). The main characteristic of the turboprop is the power that can bring to the shaft, compared to propeller engine (more than 10000 kW), and its still used today in regional transport.

2.1.2 Turboshaft

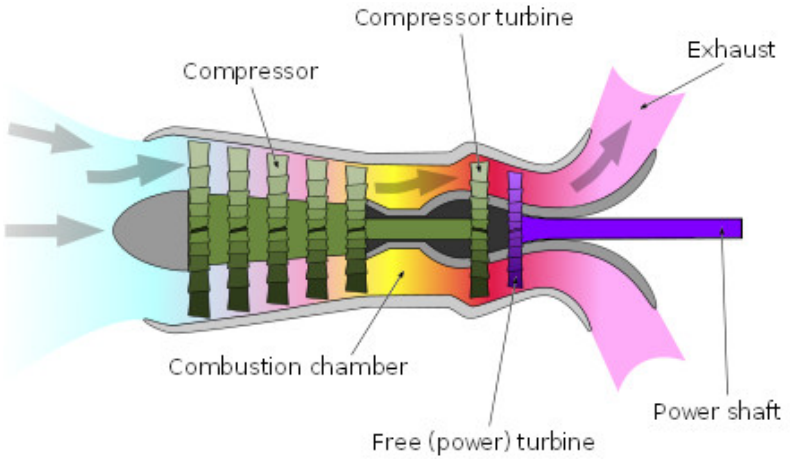

Figure 2.2: Turboshaft architecturre[4]

The turboshaft engine is the propulsion system employed in the helicopter field, and its operation is very similar to the turboprop engine. In general, the turboshaft engine normally drives a transmission which is not structurally attached to the engine. Therefore, despite to the turboprop where the loads created by a rotating propeller are supported by engine, the transmission of the turboshaft is attached to the vehicle structure in order to support the loads instead of engine. Moreover, given that helicopter rotors turns slower than an airplane propeller, is necessary to insert a gear reduction system with the purpose of adjust the rotational speed of the shaft so as to accommodate the rotor or the propeller.

2.1.3 Turbojet

The turbojet engine has been the first layout used on the jet powered aircraft, as well as the simplest version. It was adopted on German vehicle (ME 262) during

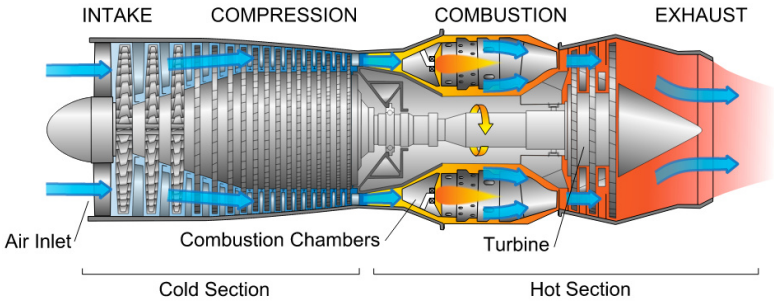

Figure 2.3: Turbojet architecturre[3]

the second world war for the first time and his simple scheme has been greatly improved during the years, leading to new configuration developments. This engine can be sketched in five modules: diffuser, compressor, burner, turbine and nozzle.

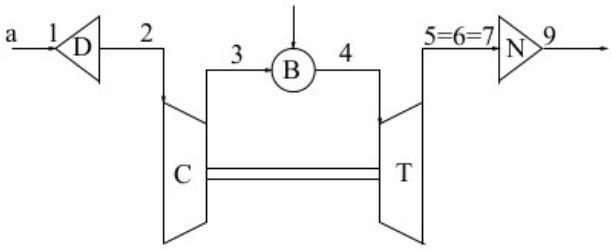

Figure 2.4: Sketch of turbojet architecture[2]

As showed in a figure 2.4, the air in atmospheric condition (a) reaches the input section (1), and in this step the air condition could change due the flow evolution on the engine outside. At this point there is the diffuser (D) that have the purpose of moving air inside the engine, increasing the static pressure, limit the total pressure losses and modify the flow conditions (such as slow the flow) in order to accommodate it the input compressor condition. While between 2 and 3 station is located the compressor, that can provide a determinate compression ratio and in particular there will be an increase of the pressure and temperature. Normally this machine is divided into HPC (high pressure compressor) and LPT (low pressure compressor). Only after is possible to find the burner (B) so as to increase the flow temperature by the provision of chemical energy by the combustion reaction. Between the 5 station and the downstream condition of the burner (4) there is a turbine, a machine which has the role to provide the amount of power needed to move the compressor. As the compressor, also the turbine can be divided in HPT (high pressure turbine) and LPT (low pressure turbine, the main topic of this thesis

work). The 6 station follow characteristics of the afterburner that takes advantage of oxygen surplus of the turbojet to make a second combustion thanks to injection of fuel of the downstream turbine. In the end, there is the nozzle (N) where the flow is expanded and accelerated.

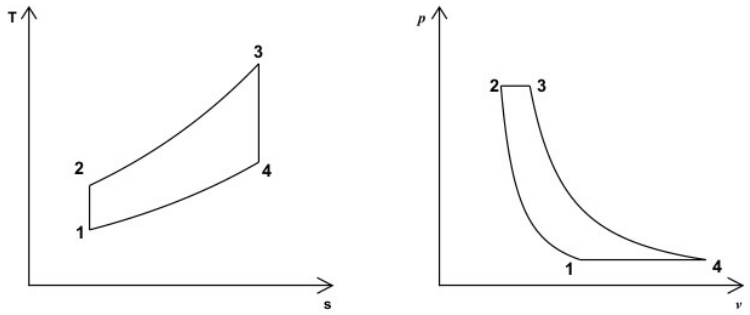

Figure 2.5: Turbogas cycle[2]

To sum up, the flow evolution through the different component describes pretty well the Brayton-joule cycle, since the latter differs between open and close cycle. In the figure 2.5, it is possible to distinguish two diagram T-s (supposing constant specific heat) and p-v, that define the transformation of heat transferred to fluid into work, through four phases of the fluid mass evolution:

1'-2' Isentropic compression, this transformation is ideal (isentropic) in fact a temperature increases at constant entropy happens. At the same time the compression causes a specific volume reduction and a pressure increase. Actually the transformation is different, in fact (1-2) no longer takes place at constant entropy but increases the latter, leading to an increase of temperature. This is how the adiabatic efficiencies are created in order to compare the ideal and real cycle.

2'-3' Heat influx at constant pressure. This transformation happens without exchange of work and lead to an increase of temperature and specific volume.

*3'-4'*Isentropic expansion, also in this case the transformation is ideal, and concerns constant entropy with a temperature decrease. At the same time the expansion causes a specific volume increase and a pressure reduction. But in a real cycle (3-4) the point in the end of heat influx (3) moving on the right side and the transformation is not ideal, indeed an increase of entropy with a temperature decrease takes place. The ratio between ideal turbine work and real turbine work is defined as adiabatic efficiency.

4'-1' The last transformation, being a close cycle, concerns a reduction of heat transfer at constant pressure. In this case the flow having a higher temperature and having to return in the initial conditions undergoes a cooling process (for the second law of thermodynamics, not all the heat provided can be processed to work). To be clear, this transformation takes place outside the engine in an open cycle, so

that the fluid gradually comes to thermal equilibrium with the environment.

The end, this engine is currently used in a supersonic field, because at flight speed (subsonic) of the commercial aviation the turbofan engine is more efficient both turboprop and turbojet engine.

2.1.4 Turbofan

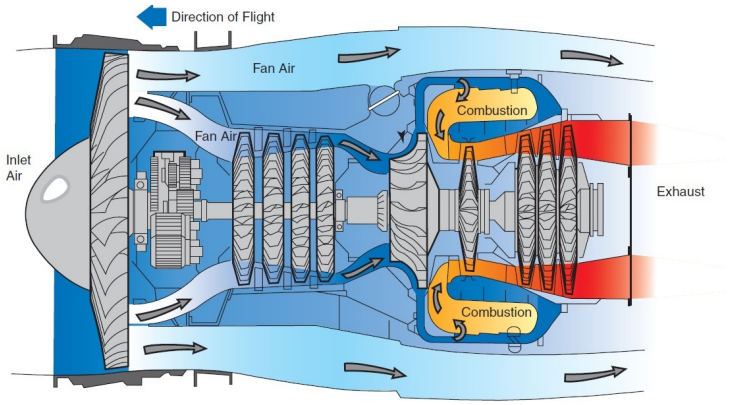

Figure 2.6: Turbofan architecturre

From the analysis made up to now, it seems clear that the introduction of turbofan engine is designed to exploit the benefits of the turbojet and turboprop engine. Observing the formula of propulsive efficiency:

$$\eta_p = \frac{1}{1 + \frac{F}{2\dot{m}_a V_0}} \tag{2.1}$$

Its possible to understand the main reason leading to introduction of this engine. In fact, the propulsive efficiency is higher with increasing of the air flow rate (ma) by the engine ingested, thereby decreasing of specific thrust. This decrease means a engine weight increase due to the fact that the compressor, combustor and turbine have to elaborate a bigger flow rate and a reduction of thermodynamic efficiency takes place. The turbofan introduction has made it possible to extract available energy at downstream of the turbine, in order to move a second turbine that gives the power to the second air flow. This process enables the reduction of the engine weight because not all the air flow crosses the turbomachinery. The secondary flow rate is compressed by the fan, it can be expanded up to environment pressure so as to contribute to the thrust.

So far, we can distinguish two flow air rates, the primary flow rate (also called flow hot rate because it passes through the combustor) and the secondary flow rate (also called flow cold rate that doesnt power any combustion process). This two

flow rates have given rise to two different configurations, turbofan with separated flows and turbofan with associated flows.

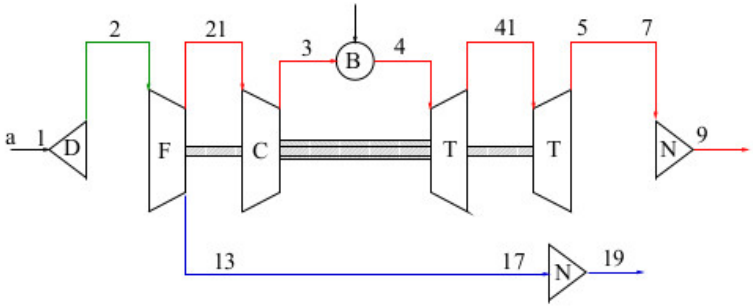

Figure 2.7: Sketch of separate-flow turbofan[2]

- Turbofan with separated flow (as shown in the figure 2.7): this engine is composed by diffuser (D), crossed by the whole flow rate (primary and secondary flow rate), as the fan (F), made up by one or more than one stages. At downstream of fan the whole flow rate is divided to flow cold rate (31) that doesnt undergo further compression in contrast to the flow hot rate (21), that will be compressed thanks to the compressor (C). At this point the primary flow rate follows the same evolution of the turbojet flow, up to exit of the first turbine (41) where the flow will be furtherly expanded due to the presence of the secondary turbine (T) that powers the fan. In conclusion the flow is speed up through the nozzle, and also the cold flow rate is expanded in a nozzle arranged right after the fan. For these engines is important to introduce a by pass ratio (BPR) that defines the ratio between the two flow rates.

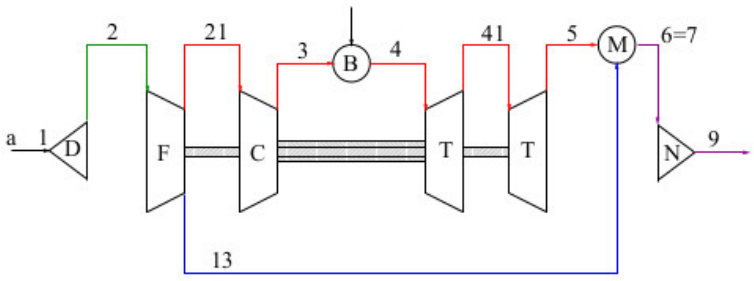

Figure 2.8: Sketch of associated-flow turbofane[2]

- Turbofan with associated flow: the main difference between separated and associated flow is that in the first case, since the flows are separated, also the temperature is different. In the second case, as shown in a figure 2.8, the secondary flow rate (13) after it has been expanded in a fan (F), it is inserted

in a mixing chamber (M) where the cold and hot flow are combined, to be expanded in a nozzle. An important constrain for the flows before going to the mixing chamber is that the two flows must have the same static pressure, so it is necessary to take an exact decision about compression ratio of fan and by-pass ratio. Considering the ratio between the two thrust (associated and separated flow) its possible conclude that is always advantageous to use the associate flow both for considerable thrust and lesser noise. But its also true that the presence of the mixing chamber means an increased engine weight.

At the end the choice between these two configurations depends on use, for instance for the commercial aviation (subsonic field), it is important low consume and raise by-pass ratio. For this reason it is used the turbofan with separated flow, because they are more lightweight and guarantee higher BPR. On the other hand if we are interested in lower BPR and lesser noise its possible to employ the turbofan with associated flow.

2.2 LPT (Low Pressure Turbine)

One of the components in aeronautical engine which has been more changed and developed during the past years is the turbine. This is due to the constant improvement of engines performances and for the goals illustrate in the lead of this report. In this paragraph LPT (low pressure turbine) will be described as component of multi-spool engine, key part of this thesis work. In particular a single spool jet engine is composed by single compressor and its associated turbine (also known as turbojet), while the multi-spool engine has been introduced to obtain higher efficiency without using the regenerative cycle, or rather, heat exchanger to preheat the workflow at the entrance of burner (component bulky and heavy). To achieve this, it is essential to provide high compression ratio which could lead to problems above all when the rotational velocity are low, because in this case the chocking condition can be reached in the last stages of compressor where the crossing sections are more narrow. The solution to this problem is to adopt a mechanical separation of compressor so as it can turn with different rotation number, eliminate tradeoff solutions (such as power and speed in a single-spool) and reach higher compression ratio.

As described in a last paragraph the turbine is the component that provides the needed power to the propeller or rotor (depending on type of engine considered) thanks to the energy extracted from the hot gases (provided from the combustion process) and their consecutive expansion to a lower pressure and temperature. In general the blade turbine, being located after the burner, are exposed to the high temperature, high stresses and high vibration effect that can create a damaging conditions, obviously avoiding a perfect blade project. In addition the latter is subjected to high turn number and this entail the stresses inception (produced

by centrifugal force and fluid forces) that could cause yielding or fracture failure. The final design of this component is a compromise between weigh and efficiency, because to preserve the same stress level at higher blade velocity, the size, hence the minimal amount of space and the weigh increases. The first stage of HPT (high pressure turbine), are exposed to the more critical condition in terms of pressure and temperature load and furthermore, it raises a lower number of stages compared to the LPT (low pressure turbine). Basically the LPT shall consist of three or six stages and is exposed to mild lower air pressure. In spite of the same thermodynamic and aerodynamic law, the difference between HPT and LPT has resulted in the design of blade turbine that differs both material and cooling system.

2.3 LPT stage

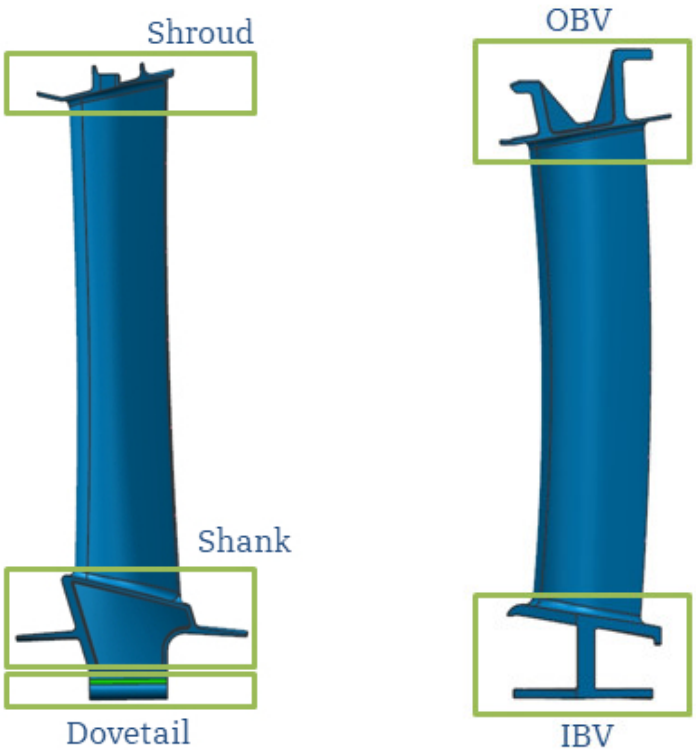

(a) Blade (b) Vane

Figure 2.9: Blade and Vane

The stator and the rotor are the two components that constitute the LPT stage and their design is especially important. In general there are three different kinds of turbines: reaction, impulse and impulse-reaction [5]. In the first, the vane is

projected in order to deflect the flow direction of gas flow without modifying the pressure, and consequently thanks to the speed up and expansion of gas on a turbine blade the reaction force will generate. Second, in this case the vane is designed so as to generate a decrease of total pressure, in order to have an impulse force on the blade turbine. In conclusion there is also the combination of the previous types of turbine. Briefly the hot gas flow expelled from burner withstand a speed up due to the convergent shape of vane, collide with blade in order to actuate the blade turbine at high velocity and in this way produces the power necessary to the compressor. Moreover both vane and blade turbine have a stagger angle higher on the tip compared to the hub, this is because not only to have the same work of gas flow along the radial dimension of blade but also to have uniform axial velocity before getting into nozzle. Another important issue concerns the optimization design of blade/disk fixing, because its from loading of root that depends the limiting rim velocity. Frequently the attachment based on multi-lobe project (fir-tree), and in this case the multiple area of contact provides to the possibility of adapting the large thermal and centrifugal stresses.

One of the essential points in the turbine design is the material choice, because the blade most of all in the first stage, has to resist centrifugal loads due high rotational speeds, bending loads caused by gas flow, in addition to thermal shock and fatigue. This is the reason therefore a lot of aeronautical enterprise like GE aviation are looking for innovative material in order to improve the blade characteristic as for instance the temperature limit. As shown in the figure 2.9 (b) the vane is composed by two element: (IBV) inner band vane and (OBV) outer band vane, whereas the blade is made up by three component, shroud that is interlocked with previous and next blade, shank end the dovetail. In both of this configurations, the airfoil is attached to the element with a fillet and furthermore the fundamental operation is the balancing, that involves an accurate assembly of all these parts.

Chapter 3

Engine Rotordynamics

The turbine may be composed by several stages, each one assembled by stator blades and rotor blades. The fundamental goal of the stator blade is to deviate the flow at the stage entrance, reaching, as a maximum, a part of the expansion, while the rotor blades interact with the fluid extracting its energy. It is fundamental distinguishing two load typologies, static and dynamic, that differ in direction and intensity variation speed in time. The static or semi static load has load frequency inferior than the lowest frequency vibration of the structure (for example the centrifugal load), while for the dynamic load we have the opposite, which is load frequencies higher than the smallest vibration frequency. This can bring to efficiency and functionality reduction.

During his life span, a rotor is subject to diverse load typologies like thermal, inertial and aerodynamic loads. The thermal load is due to the high temperature of the flow impacting on the turbine, generating a strong temperature gradient variation in radial direction. Following, the aerodynamic load defined by the interaction between fluid and structure and the inertial load, which is the centrifugal loads linked to rotation velocity of the component. All those loads act on the bladed disk, and that is the reason why it is fundamental to analyze in detail what the consequences are: deformations, tensions, shifts that could bring to critical situations and also to component breakup. Moreover, it is important to set a detailed dynamic analysis, mainly on rotors, so as to define for what frequencies the resonance phenomenon occurs, because high vibrations can lead to a structural failure. Therefore, it is necessary to define, previously in the design phase, a right architecture to minimize those phenomenons and guarantee reliability of the single components, testing them to fatigue.

Vibration phenomenons can come from two main sources, that are defined through two approaches: flutter analysis and forced response.

- *Forced response*b is one of the main worries related to bladed disk components damage, due to high cycle fatigue. The external harmonic forces that lead to

the resonance phenomenon generation, can have an aerodynamic or mechanical origin. The aerodynamic ones are due to local flow distortion that invest the blades, generating a non-conformity of the pressure range inside the turbomachinery. That phenomenon can be localized upstream and downstream of the stator blades, such as in the combustion chamber. The Mechanical forces are instead generated by bodies with no perfect symmetry.

- Flutter is a dangerous phenomenon that generates on flexible structures subject to aerodynamic forces. Mainly, it occurs as a result of the interaction between aerodynamics, stiffness, and inertial forces on a structure. There may be a point at which the structural damping is insufficient to damp out the motions which are increasing due to aerodynamic energy being added to the structure, so the component can be brought to breakup. It is possible to distinguish two flutter typologies, the classical flutter and the turbomachinery flutter. We will see them in detail in the next paragraphs.

3.1 Forced Responce

The harmonic forcer, as just explained, could be caused by the hot gas movement getting out from the burner and entering the turbine, origin of the cyclical exciting between stator and rotor.

The forcer applied on a system can be seen as an impulse during each blades revolution. This impulse has not an infinitesimal duration, therefore is not insignificant compared to revolution period.

It is fundamental then to avoid the resonance phenomenon, in which natural frequencies of the system coincide with aerodynamic frequency, because it can generate vibrations causing components damage. The stress frequencies can be described by a parameter that put into relationship the forcer pulsation and the rotational velocity of the flow, called Engine Order (EO).

$$EO = \frac{\omega}{\Omega} \tag{3.1}$$

We can define the static or rotating forces based on the reference system chosen, that can be a stator based reference frame or rotor based reference frame. To define the phenomenon from the mathematical point of view, we can take into account a simplified case, with 4 blades excited by a forcer

$$\begin{cases} f_{\theta^*}(t) = F_0 cos(\omega t) = F_0 cos(N_b \Omega t) \\ f_{\theta \neq \theta^*}(t) = 0 \end{cases} \tag{3.2}$$

Where ω is the forcer frequency,Ω the natural frequency, while N_b is the blade number. In this case we consider a harmonic forcer that excites the bladed disk in a determined point of the space, identified as θ

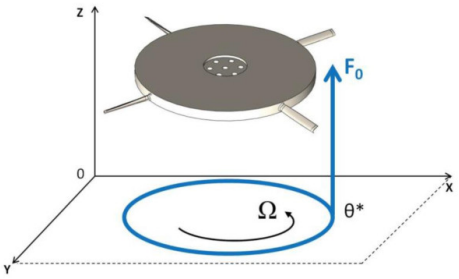

Figure 3.1: Forcer F_0 applied to the rotating disk at the θ^* angle[6]

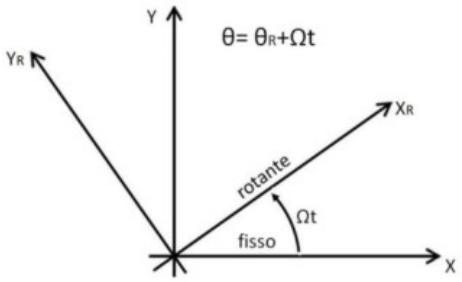

Figure 3.2: Variable change [6]

Considering a reference system fix in space, the harmonic forcer can be decomposed in Fourier series, with n representing the harmonic index:

$$f_\theta(t) = \frac{F_0}{\pi} \sum_{n=1}^{\infty} cos[n(\theta - \theta^*)]cos(\omega t) \tag{3.3}$$

While considering a rotating reference system, with a variable change as shown in figure 3.2 we have:

$$\begin{aligned} f_{\theta,R}(t) = \frac{F_0}{2\pi} \sum_{n=1}^{\infty} & cos[(\omega - n\Omega)t]cos(n\theta_R) + sin[(\omega - n\Omega)t]sin(n\theta_R) + \\ & cos[(\omega + n\Omega)t]cos(n\theta_R) - sin[(\omega + n\Omega)t]sin(n\theta_R) \end{aligned} \tag{3.4}$$

Observing the above mentioned equation, it is possible to identify two forcers: forward forcer, with pulse $\omega_f = \omega - n\Omega$ and backward forcer with pulse $\omega_b = \omega + n\Omega$.

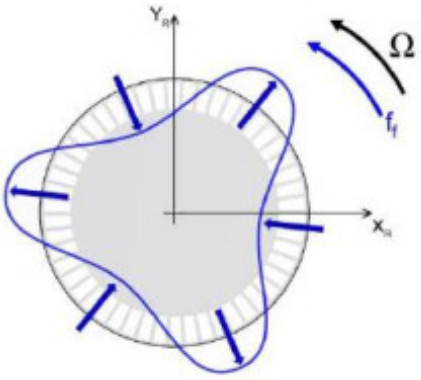

Figure 3.3: Forward forcer[7]

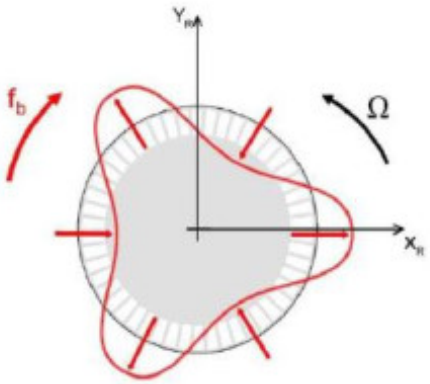

Figure 3.4: backward forcer[7]

Considering those premises, it is possible to claim that in a rotating reference system, with an established harmonic value of the Fourier series n (for instance, considering n=2) the component will be excited by two different EO:

$$\begin{cases} \omega_b = \omega + n\Omega = \Omega(N+n) = \Omega(4+2) = 6\Omega = EO_b\Omega \longrightarrow EO_b = \frac{\omega_b}{\Omega} = 6 \\ \omega_f = \omega - n\Omega = \Omega(N-n) = \Omega(4-2) = 2\Omega = EO_f\Omega \longrightarrow EO_f = \frac{\omega_f}{\Omega} = 2 \end{cases} \tag{3.5}$$

EO_b and EO_f, are the EO that, in the rotating reference system, excite the disk. Therefore, as we can observe, in this case the curves inclination is expressed by the EO, unlike the static case where only the forcer$EO = 4$. One of the tools used to identify those aspects is surely the Campbell diagram, that puts into relationship the natural frequencies of the structure in function of the rotating speeds.

3.1.1 Campbell Diagram

As laid down in the previous paragraph, the Campbell is a diagram where in the x-axis there is the number of turns, while in the y axis the frequencies, and it is intended to identify the resonance points. Considering a fixed velocity configuration, and imagining to set a straight line, it is possible to determine the intersections (according to the number of EO) on the diagram and each of these points can correspond to likely resonance conditions. Considering, instead, working on a pulse with fixed excitation $\omega_{nat,1}$,the intersection with possible EO (possible resonance conditions), happens at different rotation speeds. Anyway, in the rotating reference system it is possible to identify the real frequencies [6].

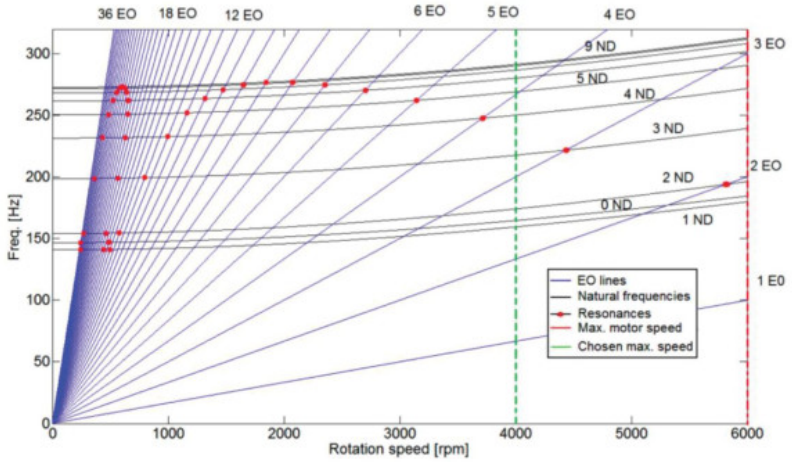

Figure 3.5: Campbell diagram[6]

As shown in the figure 3.5, the Campbell diagram represents Engine Order and natural frequencies of the modes. It is interesting to see the intersection between the two evolutions that define the crossing (highlighted in red). Those represent possible resonance points that can be more or less dangerous depending on the time of condition perduring and on the amplification level [8]. The Campbell diagram also shows the velocity range that defines the operational condition of the engine (green and red lines), where crossing points should be avoided. Eventually, in those diagrams, also the thermal effect (softening) and the centrifugal stiffening must be taken into account, so the natural frequencies can have a variable behavior for different rotation velocities.

3.1.2 Resonance

The resonance phenomenon occurs when the forcer frequency of the bladed disk coincides with a natural frequency of the disk. As follows, the mathematical development of the issue, to get the resonance formulation. The first step is to consider a generic mode n:

$$y_n(\theta, t) = -y_n cos(\omega_n t + ND\theta) \tag{3.6}$$

With fixed rotation speed, natural frequency ω_n and angular coordinate θ. If the stiffening phenomenons are not considered, the harmonic frequencies can be considered fixed compared to rotation velocity. The following step is to break down the periodic forces on the blades in its harmonic components (trough Fourier)

$$f(\theta, t) = F_0 + \sum_{k=1}^{\infty} F_k sin[k(\omega t + \theta)] \tag{3.7}$$

Where t means time andF_k the width of the $k-th$ harmonic. Following, the work during the period T made by the $k-th$ harmonic of the forcer on the mode with nodal diameter n:

$$W = \int\int f dy d\theta = \int\int f \frac{dy}{dt} dt d\theta = \int_0^2 \pi \int_0^T f(\theta, t) \frac{\partial y_n(\theta, t)\Omega}{\partial t} \frac{\Omega}{2\pi} d\theta dt \tag{3.8}$$

At this point, it is possible to define the resonance as the condition in which work described is positive, as in the following mathematical formulation:

$$W = \begin{cases} \pi \Omega F_k y_n, per \omega_n = k\omega ek = n \\ 0, per \omega_n \neq k\omega ek \neq n \end{cases} \tag{3.9}$$

In this formulation it is possible to highlight two conditions. The first one is the traditional definition of resonance (as used so far), while the second condition defines the equality between nodal diameter and harmonic force. Basically, only

when a work storage occurs the resonance condition is verified. The relationship defining the Engine Order and stimulate, in resonance, a vibration mode with nodal diameter n:

$$\begin{cases} EO = n \\ EO = N_b \pm n \end{cases} \tag{3.10}$$

That in general can be written as follows:

$$EO = mN_b \pm n, \qquad \forall m \in N \tag{3.11}$$

If the forcer has a force corresponding to the vibration mode, the EO is equal to nodal diameter and for that reason a situation of resonance verifies when frequency equals to the natural one. The exciting effect of the forcer doesnt have the same effect with the variation of the nodal diameter, because the forcer is orthogonal to all of the modes [9].

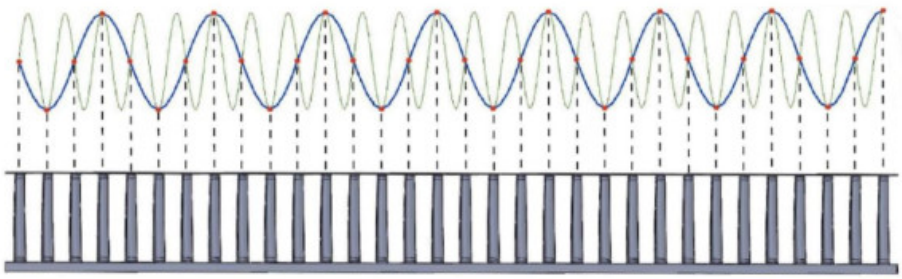

Figure 3.6: Aliasing phenomenon EO 24 $\longrightarrow$ 8. [9]

Another important phenomenon is Aliasing, which is the capacity of the EO, defined in the second equation, that achieves stimulating the mode with odal diameter n in resonance. An example is shown in figure 3.6 where the forcer is discretized with $E = 24$ through the turbine blades. It is clear that, in this case, for the aliasing phenomenon the blades dont perceive a forcer with $EO = 24$ (green) but they work as they were excited by a forcer with $EO = 8$ (blue).

3.1.3 Mistuning

The issues treated up to now are based on the hypothesis that a rotor was perfect (tuned), with perfectly identical sectors. This is not possible in real life, there are always differences linked to, for example, to its use or fabrication variations. Those imperfections (mistuning casual) cause the cyclic symmetry loss, with consequent variations of the dynamic features, generating higher responses that the ones calculated in tuned conditions [10]. It is important to highlight that a mistuning weighted selection (intentional mistuning) could allow the aeroelastic stability

improvement in the tuned system. This issue is explained in figure 3.7, where it is shown that mistuning influences the forced response of a bladed disk, with following comparison with experimental data.

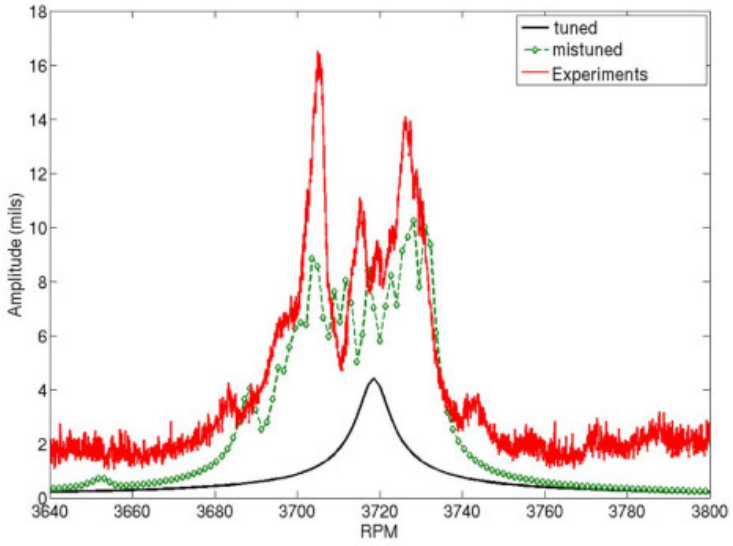

Figure 3.7: Forced responce - Tuned and Mistuned, comparison with experimental data [10]

3.2 Flutter

The flutter is the complex of self-sustained and self-excited vibration of structure, where the natural frequencies of the system generate its vibration modes. In general this physical phenomenon concerns the onset divergent oscillations on the elastic structure, immerse in a stream air. The critical parameters with an established geometry are the velocity, indeed when $V = V_{cr}$ the aerodynamics oscillations are supported (limit of instability), while for $V<V_{cr}$ the aerodynamic oscillations are damped and at finally the condition $V>V_{cr}$, where the aerodynamic oscillations are heightened. Mathematically speaking, for these types of phenomenons, the eigenvalues of the aeroelastic system are analyzed in different conditions. Following, as shown in a figure 3.8, it can be observed the airfoil with degrees of freedom, and the relative equation of motion:

$$\begin{cases} m\ddot{h} - S_\theta\ddot{\theta} + Kh = L \\ -S_\theta + I_\theta\ddot{\theta} + K_\theta = M \end{cases} \tag{3.12}$$

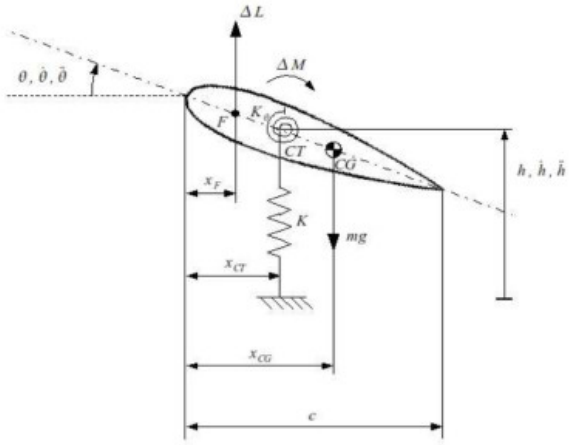

Figure 3.8: Profile section with 2 dofs

The second order of static moments are defined as:

$$S_\theta = \int_m (x - x_{CT})dm \qquad I_\theta = \int_m (x - x_{CT})^2 dm \tag{3.13}$$

Considering the quasi-steady approach for the lift and moment, its possible to introduce only one parameter dependent from time:

$$\alpha(t) = \alpha_0 + \theta(t) - \frac{\dot{h}}{V_\infty} \qquad C_L(t) = C_{L\alpha}\alpha(t) \tag{3.14}$$

As a result the aerodynamics moment and lift can be expressed as:

$$\begin{cases} L(t) = q_\infty c C_{L\alpha}(\theta - \frac{h}{V_\infty}) \\ M(t) = q_\infty c^2 CL\alpha(\theta - \frac{h}{V_\infty})(\frac{x_{CT}}{c} - \frac{1}{4}) \end{cases} \tag{3.15}$$

Where x_{CT}, is the dimensionless coordinate of shear center, c is the chord of the aerodynamic profile and q_∞ is the dynamic pressure. Following, the matrix format is introduced:

$$[M]\ddot{q} - [D_{AER}]\dot{q} + ([K] - [K_{AER}])q = 0 \tag{3.16}$$

In this case no strength or external moment have an effect on system, and moreover the KAER is the aerodynamics matrix:

$$[K_{AER}] = q_\infty c C_{L\alpha} \begin{Bmatrix} 0 & 1 \\ 0 & c(\tilde{a}_{CT} - \frac{1}{4}) \end{Bmatrix} \tag{3.17}$$

Introducing the harmonic response it can be acquired the eigenvalues ω and the eigenvectors $\bar{q}$ of the system, in order to obtain the flutter velocity. Definitively the flutter instability is introduced from sign change of eigenvalue real part. Basically when the real part becomes positive, the oscillation starts to amplify.

The wing structures and the turbomachinery blades answer in a different way to this phenomenon, and it mainly depends on the relationship between the mass of the body and the one of the fluid. In particular frequently the wing structure introduces a flex-torsional flutter due to their lightness, whereas the turbomachinery blades response with single mode introduces frequency close to their free response [11]. The oscillations could raise in short time, if the system was not conveniently damped, and this is one of the reasons that define the danger of these phenomena. Essentially this is due to the fact that, when the vibration is activated, the energy that the structure can absorb is a lot smaller compared to the kinetic energy of the flow that feeds the vibration themselves.

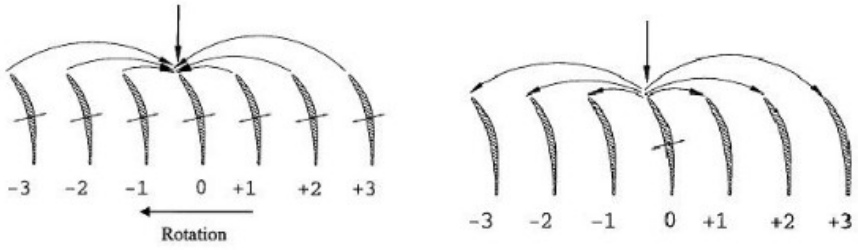

Figure 3.9: Unsteady aerodynamic influences acted on blade[12]

The main difference between classic flutter and turbomachinery flutter is due to a range of factors, and one of the most important is the requirement that the blade behavior is influenced from the consecutive blades. In the figure 3.9, its a possible to observe the interaction between consecutive blades, and in particular, the blade motion generated by the unsteady aerodynamic loads on the adjacent blades. Many other factors can condition the aerodynamic problem within turbomachinery, and the more considerable are [13]:

- Pressure loads on blades are influenced by collisions
- Reduced frequency, used to distinguish the unsteady flow conditions and the flow quasi-steady conditions, defined as:

$$k = \frac{c\omega}{2V} \tag{3.18}$$

- Inlet-outlet thermofluid-dynamic conditions, that influence the aerodynamic damping

- The alteration of interface loads and the modalshapes due to the shroud presence that introduce a damping generated by friction.
- Interblade phase angle is a relationship that represents the effect between consecutive blades:

$$IBPA = \sigma = 2\pi\frac{n}{N} \tag{3.19}$$

- Mistuning: as already mentioned in the previous paragraph the pattern of mistuning introduction has a stabilizing effect on aero elastic problem.

3.3 Modal Analysis

The reliable design of turbomachinery blade starts from the natural frequency analysis, because the main reasons of blade failure are due to the metal fatigue that is introduced by the variation of the aerodynamic loads. During the years, throughout different studies, it has been possible to understand that the natural frequency analysis defines a various answer depending on the fact that the design is based on single blade or an assembly where a group of blades are connected by shrouding [14]. This kind of assembly introduces many more natural frequencies and modes that do not exist in the single blade analysis, and this new approach has been useful for designers to build more reliable blades. A Second important steps concerns the insertion of the disk that, as demonstrated by several studies, influences the blade dynamic behavior.

The basic dynamic properties of structure are represented by mode shapes and natural frequency, and if these data are obtained accurately, they provide the structural properties about interest modes. The properties of mass, damping and stiffness of this modes determinate the matrices, in the real boundary conditions of the structure. This data can be used in a FE (finite element), in order to define the subsequent problem solving with more optimum dynamic response [15]. In such a way the FE analysis determinate the structural dynamic properties as well as the natural frequency and the modal shapes. The finite element software used in this work thesis, NASTRAN and Ansys Workbench, are programmed to solve the equation of motion:

$$[M]\ddot{x}(t) + [C]\dot{x}(t) + [K]x(t) = f(t) \tag{3.20}$$

Where $[M], [C]$ and $[K]$ are the mass, damping and stiffness matrices, while x and $f$are respectively the DOFs and external forces vector. The first part of problem solution inspects the undamped system solution with no external excitation:

$$([K] - {\omega_i}^2[M])u_i = 0 \qquad i = 1, ..., N \tag{3.21}$$

The solution to this equations set out the natural frequency (eigenvalues) and the non-damped mode shapes (eigenvectors). Basically, the modal analysis advantages can be summed up in this two points:

- The rapid and effective procedure for the structural dynamic properties data acquisition.
- This procedure allows the resolution of the large structural dynamic equation, being able to reduce complex matrix equations.

3.4 Modeshapes

In the analysis of the vibration modes, it is important to define the vibration frequencies, but at the same time it is necessary and equally essential, to identify the modal shapes associated. The cyclic symmetric structure presents several particular vibration modes called nodal diameters (ND) and nodal circumferences (NC). The first case is identified by straight lines through the disk center and it is characterized by the null modal displacement. Whereas the second case (NC) defines the concentric circumference, where the points on them not show displacement.

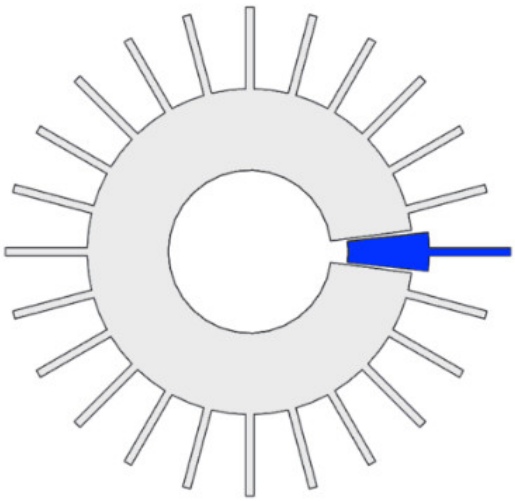

Figure 3.10: Sector of a bladed disk in cyclic symmetry

Basically, the blade-disk structure has the same angle θ for each radial and axial position, and this is due to the cycle symmetry. In particular it is identical at $(\theta + n\phi_0)$, considering that ϕ_0 is $\frac{2\pi}{N}$ and N define the number of blades. Anyway, the number of nodal diameters is occurred in two different way, depending on the number of sector N, which is $\frac{N}{2}$ if it is even and $\frac{N-1}{2}$ if it is odd.The figure 3.10,

shows the blade disk in cycle symmetry, whereas the figure 3.11 [7], describes the deflected shapes of a blade disk with 12 sector.

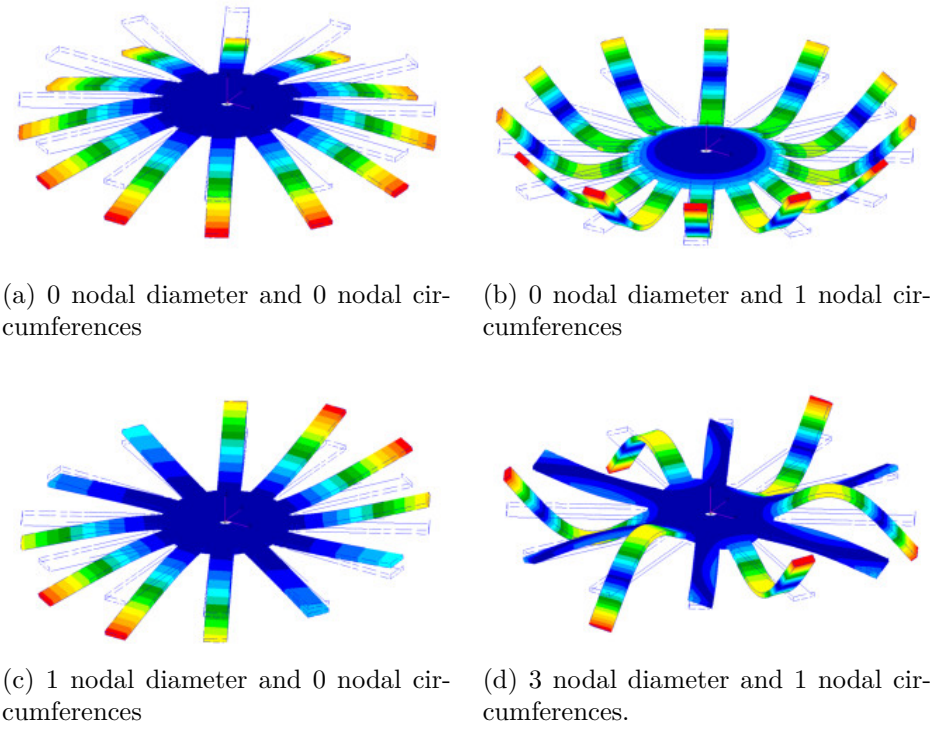

(a) 0 nodal diameter and 0 nodal circumferences

(b) 0 nodal diameter and 1 nodal circumferences

(c) 1 nodal diameter and 0 nodal circumferences

(d) 3 nodal diameter and 1 nodal circumferences.

Figure 3.11: Deflected shapes with nodal diameters and nodal circumferences

The nodal diameters allow to differ the vibration mode as follows:

- Rotary modes: these are modes described by pairs real eigenvectors (steady-state) that introduce a modal squareness borne out by the null scalar product. In this case the phase between two steady eigenvectors, in the two modes is the opposite, (ϕ_{1x} and $-\phi_1$) involve in this way the opposite rotation of the modes.

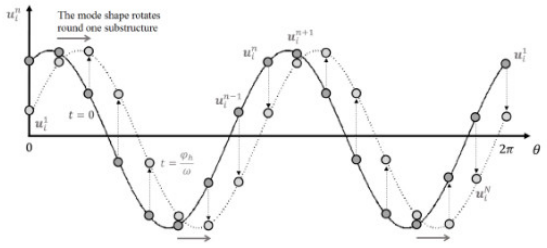

Figure 3.12: Rotating mode, the position of the peaks shifts in time

- Steady modes: these modes are described by standing wave, where all sector vibrate with the same level of phases and amplitude. It presents only real eigenvectors.

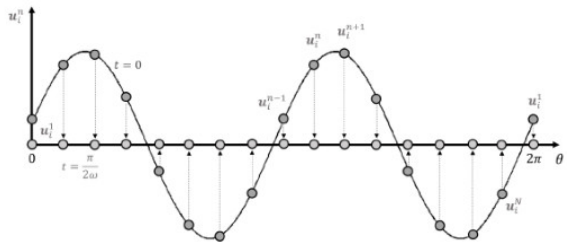

Figure 3.13: Standing wave, the peaks don't change position

It is important to stress, however, as the Inter Blade Phase Angle IBPA, can delimit the periodicity of vibration modality (ND). Indeed, the IBPA can assume negative value, thereby counterclockwise rotating modes, or positive value corresponding to clockwise rotating mode [8]. The ψ value can assume the following value:

$$\begin{cases} l\psi \in [-\pi, -\frac{2\pi(\frac{N}{2}-1)}{N}, ..., -\frac{4\pi}{N}, -\frac{2\pi}{N}, 0, \frac{2\pi}{N}, \frac{4\pi}{N}, ..., \frac{2\pi(\frac{N}{2}-1)}{N}, \pi] & \text{N } \textit{even} \\ \psi \in [-\frac{2\pi(N-1)}{N}, ..., -\frac{4\pi}{N}, -\frac{2\pi}{N}, 0, \frac{2\pi}{N}, \frac{4\pi}{N}, ..., \frac{2\pi(N-1)}{N}] & \text{N } \textit{odd} \end{cases} \tag{3.22}$$

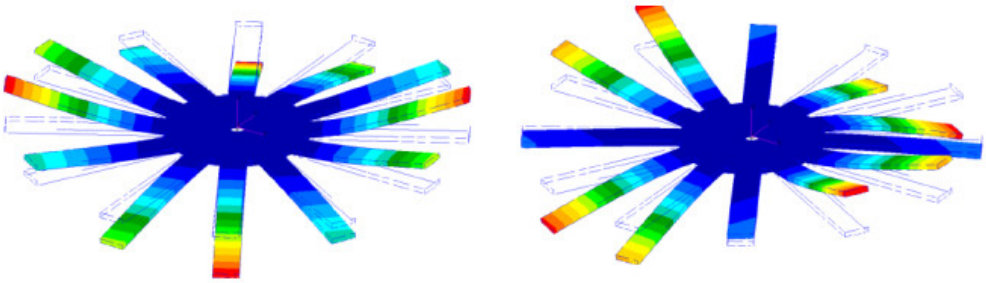

(a) First deflected shape (b) Second deflected shape

Figure 3.14: Deflected shapes of a mode with ND = 2

Type modes (a): IBPA and ND assume null value, and the mode is composed by a single real eigenvector (positive).

Type modes (b): the vibration in in anti-phase and the mode is characterized by a single real eigenvector (negative). In this case the nodal diameter has to be $\frac{N}{2}$, in order to have $\psi = \pm\pi$, and consequently the number of blades has to be even.

Type mode (c): in this case it is possible analyze a rotating mode with a complex eigenvector. The vibration is in different phase with a consecutive sector.

3.4.1 Modal Families: FREND Diagram

The blade-disk system introduces several vibration modes that differ for nodal diameter. Every one of this vibration modes fitting the modal shapes as many as the numbers of degrees of freedom. Greater nodal diameter determinate the globally system more stiff and higher vibration frequency. The easier deformed configurations play an important role from an engineering point of view, because most effected by breaks or unsteady structure phenomenon. In practice its important to focus on the first frequencies of a nodal diameter and these are defined as *modal families*. Normally the modal families are shown through a diagram called FREND (FREquency-Nodal-Diameter), where the x and y axis are composed by nodal diameter and Natural frequency of modes respectively.

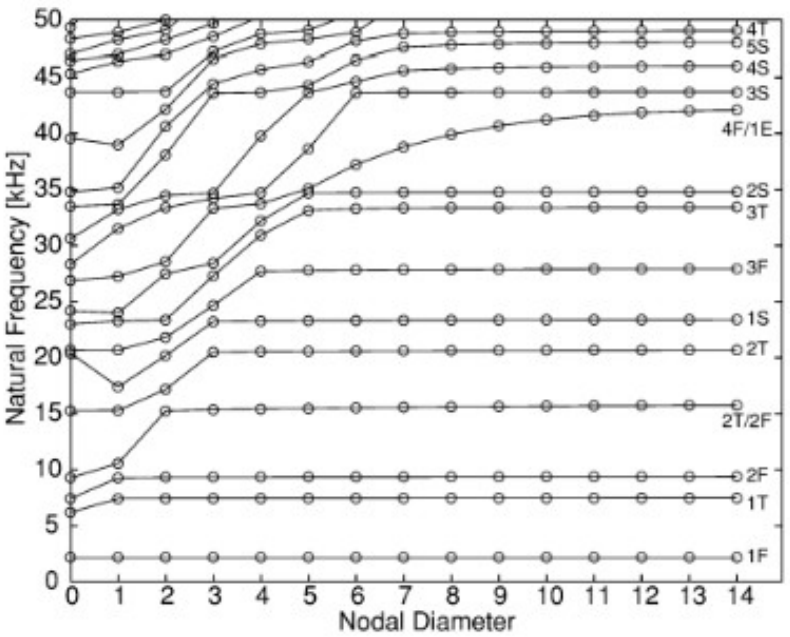

Figure 3.15: Example of FREND diagram [7]

As shown in a figure 3.15, the typical trend of this diagram concerns a growing evolution for low nodal diameter and an asymptotic evolution for high value. The

first vibration modes are mainly connected to the disk modes, in other words, in this case the disk is deformed leaved the blade undeformed Otherwise there will be an opposite situation where the disk is highly stiff, and the blade is deformed.

In the following are shown much more clearly the most relevant modal families. Edgewise (1EW), is a translation quasi-stiffness in hoop direction of the shroud; flapwise (1FW), is bending in axial direction with maximum arrow on the top of blade; Bending mode, is a bending with maximum arrow at the medium radius of the blade and torsional mode, provide a double lobe deformation.

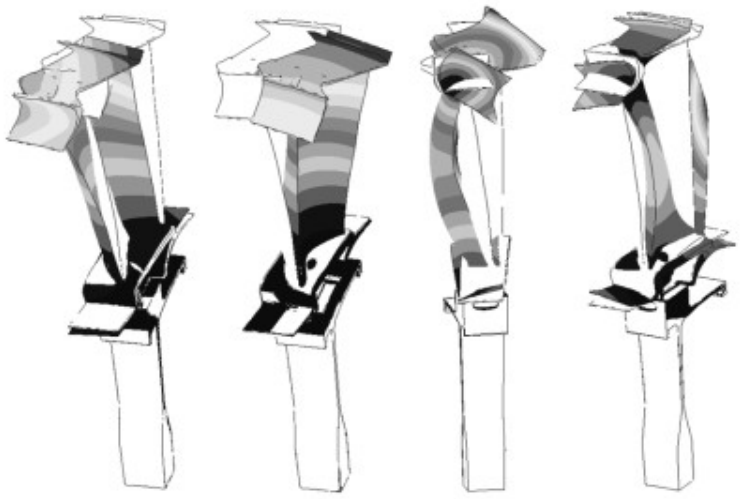

Figure 3.16: Example of mode shapes for a blade: edgewise, flapwise, bending and torsion

3.5 Cyclic Symmetry

One of the key points of this chapter is the bladed disk modeling. The followed process will be defined to carry out the analysis on the whole structure. Essentially the issue connected to the whole structure analysis depends on the high degree number freedom that makes the analysis impossible. In particular this is due to the limit of memory of computer or the maximum number of nodes that the software can manage. The solution to this problem, consists in utilizing some techniques that reduce the number of DOFs, for instance the Reduced Order Modelling (ROM)[8]. In other words, the cyclic symmetric allow to define the dynamic analysis taking into account a single sector and not the whole structure.

From the mathematical point of view, considering the discretization of equation 3.20, and eliminating the damping contribution from it, the cyclic symmetric bodies can be represented as symmetric structure with circulant block. The circulant

matrix can be defined as:

$$[M] = \begin{bmatrix} [M_0] & [M_1] & [M_2] & \dots & [M_2] & [M_1] \\ [M_1] & [M_0] & [M_1] & \dots & [M_3] & [M_2] \\ [M_2] & [M_1] & [M_0] & \dots & [M_4] & [M_3] \\ \vdots & \vdots & \vdots & \ddots & \vdots & \vdots \\ [M_2] & [M_3] & [M_4] & \dots & [M_0] & [M_1] \\ [M_1] & [M_2] & [M_3] & \dots & [M_1] & [M_0] \end{bmatrix} \quad x = \begin{Bmatrix} \{{x_1}^S\} \\ \{{x_2}^S\} \\ \{{x_3}^S\} \\ \vdots \\ \{{x_{N-1}}^S\} \\ \{{x_N}^S\} \end{Bmatrix}$$

$$[K] = \begin{bmatrix} [K_0] & [K_1] & [K_2] & \dots & [K_2] & [K_1] \\ [K_1] & [K_0] & [K_1] & \dots & [K_3] & [K_2] \\ [K_2] & [K_1] & [K_0] & \dots & [K_4] & [K_3] \\ \vdots & \vdots & \vdots & \ddots & \vdots & \vdots \\ [K_2] & [K_3] & [K_4] & \dots & [K_0] & [K_1] \\ [K_1] & [K_2] & [K_3] & \dots & [K_1] & [K_0] \end{bmatrix} \quad F = \begin{Bmatrix} \{{F_1}^S\} \\ \{{F_2}^S\} \\ \{{F_3}^S\} \\ \vdots \\ \{{F_{N-1}}^S\} \\ \{{F_N}^S\} \end{Bmatrix} \tag{3.23}$$

Where $[K_i]$ and $[M_i]$ are square matrix with n dimension. At this point, the nodes nodal displacement of the sector can be defined as sum of cosine and sine components, introduced the Fourier transformation. Moreover, considering the change coordinates, the equation 3.21 is expressed in the following way [16]:

$$\left(\begin{bmatrix} [\bar{K}_0] & 0 & 0 & \dots & 0 & 0 \\ 0 & [\bar{K}_1^C] & 0 & \dots & 0 & 0 \\ 0 & 0 & [\bar{K}_2^C] & \dots & 0 & 0 \\ \vdots & \vdots & \vdots & \ddots & \vdots & \vdots \\ 0 & 0 & 0 & \dots & [\bar{K}_2^S] & 0 \\ 0 & 0 & 0 & \dots & 0 & [\bar{K}_1^S] \end{bmatrix} - {\omega_i}^2 \begin{bmatrix} [\bar{M}_0] & 0 & 0 & \dots & 0 & 0 \\ 0 & [\bar{M}_1^C] & 0 & \dots & 0 & 0 \\ 0 & 0 & [\bar{M}_2^C] & \dots & 0 & 0 \\ \vdots & \vdots & \vdots & \ddots & \vdots & \vdots \\ 0 & 0 & 0 & \dots & [\bar{M}_2^S] & 0 \\ 0 & 0 & 0 & \dots & 0 & [\bar{M}_1^S] \end{bmatrix} \right) \begin{Bmatrix} \{{a_0}^C\} \\ \{{a_1}^C\} \\ \{{a_2}^C\} \\ \vdots \\ \{{a_2}^S\} \\ \{{F_a}^S\} \end{Bmatrix} = \{0\} \tag{3.24}$$

The 3.24, allows to evaluate the single DOFs sector and a specific nodal diameter to define the eigenvalues and eigenvectors. Each sector introduces two symmetric cyclic symmetric region, shroud and disk. As show in the following part, its possible to observe the DOFs vector $\{x^S\}$ of the sector and the exciting force vector $\{F\}$, where the subscript L and R locate the adjacent sector position.

$$\{x^S\} \begin{Bmatrix} \{{x_L}^S\} \\ \{{x_I}^S\} \\ \{{x_R}^S\} \end{Bmatrix} \qquad \{F\} = \begin{Bmatrix} \{F_L\} \\ \{F_I\} \\ \{F_R\} \end{Bmatrix} \tag{3.25}$$

Examining only one sector, as shown on a figure 3.17, it is necessary to introduce the relationship between the external right and left points of DOFs

$$\{{x_R}^S\} = e^{i\psi} \{{x_L}^S\} \tag{3.26}$$

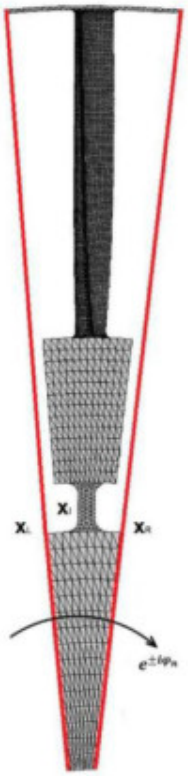

Figure 3.17: Single sector of a bladed disk

In this case, its important to highlight to evaluate the phase shift angle (IBPA) fixed of the sector. Another main point to consider is the perfect mesh comparison on the contact faces, in order to have this DOFs vector:

$$\{x^S\} = \begin{Bmatrix} \{{x_L}^S\} \\ \{{x_I}^S\} \\ e^{i\psi}\{{x_R}^S\} \end{Bmatrix} \tag{3.27}$$

At last also the stiffness and mass matrices change, following the logic just expressed, in order to have this eigenproblem:

$$\left\{([K^S(\psi)] - \omega^2[M^S(\psi)])\right\} \begin{Bmatrix} \{{x_L}^S\} \\ \{{x_I}^S\} \end{Bmatrix} = \{0\} \tag{3.28}$$

To evaluate all the modal shapes, the eigenproblems has to be resolved to the change of the ψ value.

Chapter 4

Design of LPT Stage

Currently, the majority of the modern gas-turbine engine use a multi-shaft design with separate low-pressure turbines (LPT), and high-pressure turbines (HPT). The LPT, in case of turbofan engine, are used to power the fan and/or simply power a low-pressure compressor. They often are directly connected to a rotor-drive for rotary-wing and power applications. The LPT stage is the most important component for determination of efficiency and performance of the whole engine. The new generation turbines work with efficiency which can reach about the 90%, therefore its very difficult to perform an increase of efficiency through an improvement of LPT aerodynamic design. The weight of LPT can reached the 30% of the total weight of an aircraft engine and this is due to large diameter of LPT used to obtain the maximum power at a fixed rotational speed. This is the reason why many of the business investments are going in the direction of improving engine design through weigh reduction. Even NASA through a study, has shown how a 10% weight reduction of the LPT turbines is more effective than in other engine components to reduce the operating cost, considering large transport aircrafts engines [17]. For the above mentioned reasons the design of the LPT stage plays the major role on the overall engine performance.

In general, the design of new generation turbines follows a complex procedure that is decided into two main parts: aerodynamic and structural mechanics.

- The aerodynamic procedure charged to maximize efficiency of the blade and therefore the conversion of the energy contained in the flow into mechanical power transferred to the shaft. This energy conversion is possible through two rows of blades, a *stator* followed by a *rotor*.

- Mechanical structural is the study of component resistance to static and dynamic loads, to which turbine blades are generally subjected during the operating life.

A further study concerns the analysis of the fluid structure interaction, in such a way as to define the potential unstable vibratory phenomena that can verify

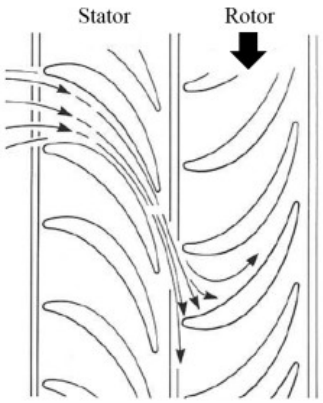

Figure 4.1: Turbine driven by the impluse of the gas flow[18]

under certain conditions. These are the classical conditions in which the vibrations induced by the rotation are amplified by the flow. As a consequence, the flutter analysis guarantees the absence of such conditions within the engine operating range. Finally, the preliminary design of LPT, through the consideration of some input parameters, sets the goal of:

- Roughly define the cross-section based on the global inlet/outlet pressure drop (figure 4.2).
- Introducing an outlining the engine dimensions
- Power output

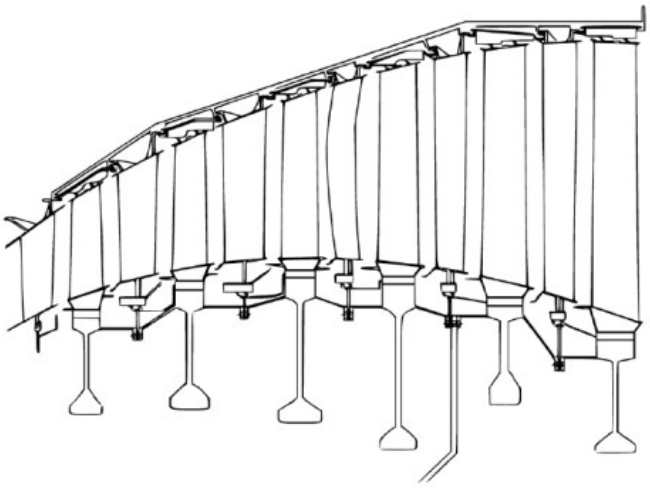

Figure 4.2: LPT cross-section[8]

4.1 Aerodynamic Design

The aerodynamic design is an important aspect in the preliminary study of LPT, since in this phase the shape of the airfoil blade is defined with maximum efficiency, so as to obtain the desired expansion ratio. This process starts with the careful determination of the turbine flowpath. At a certain working condition known as design point, the flowpath defined the channel traveled by the air flow while expanding. This is described, from a geometric point of view, on the 2D-sketch by a collection of corner points representing the projection of the engine cross section of the maximum size of vane or rotor blade aerodynamic profile [18].

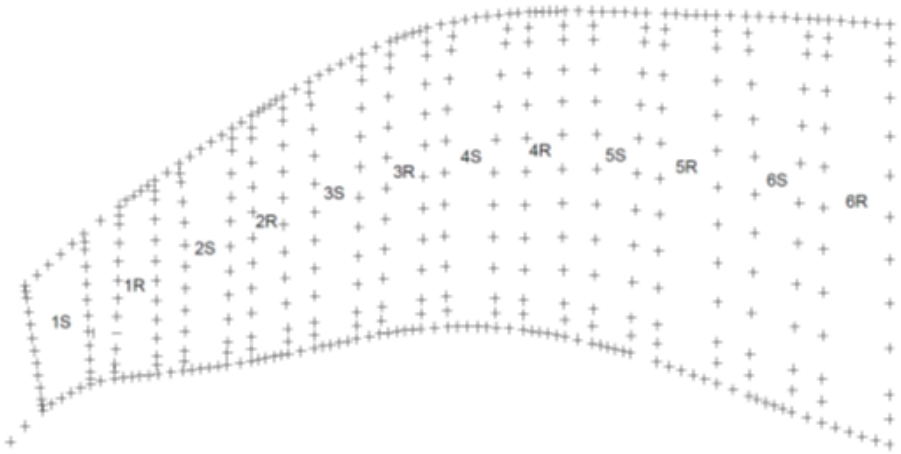

Figure 4.3: Flowpath of a 6 stages LPT: the sketch identifies the position and maximum size of R (rotor) and S (stator) blade profiles

The aerodynamic design is composed by three main parts: 1D optimization process, base 3d profile and optimization.

- *1D optimization process.* This phase starts from the subdivision of the LPT into stages and each of them can be furtherly divided into sectors, with the purpose of meeting the requirements arising from conceptual design of the engine. This first step is based on the concept that a single stage cannot produce an enough large pressure drop to match the global input/output pressure ratio. The velocity triangles (figure 4.4) define the fluid path through the machine and are used to determinate important characteristic of the bi-dimensional airfoil as leading and trailing edge orientation. In order to guarantee the same work process of the air flow, a different angle of stagger is inserted along the length of the blade in different radial coordinates.
- *Base 3D profile.* The Avio Aero know-how provides a series of empirical correlations in order to elaborate the results obtained by the 1D project. The aim is to build the 3D shape of the airfoil that best meets the performance

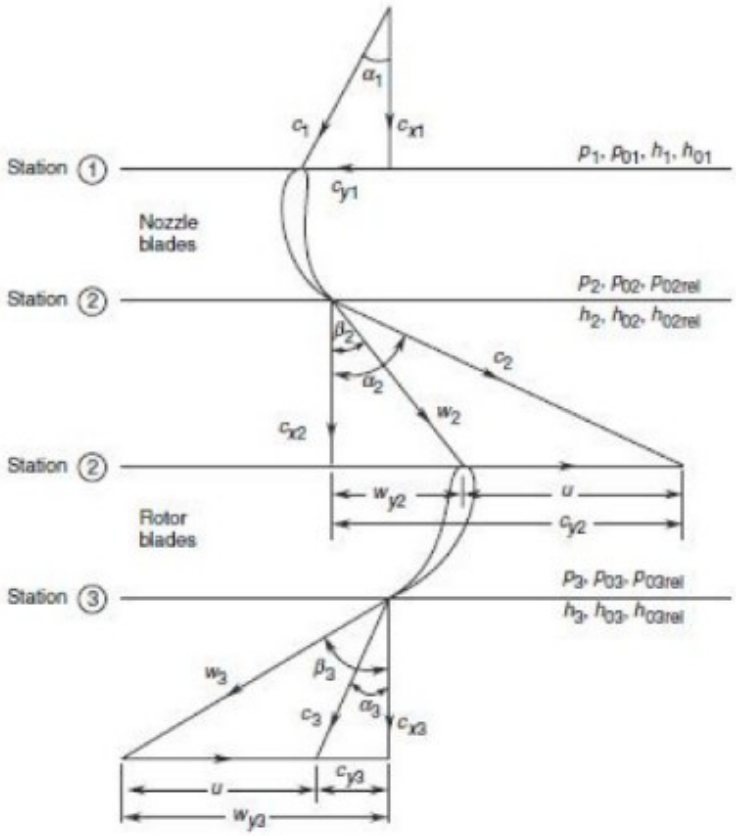

Figure 4.4: Velocity triangles of a turbine stage. The velocity in the coordinate system rotating with the rotor is w, whereas c define the speed in the steady reference system. The leading and trailing edges geometry defines the optimal flowpath.[8]

requirements. After the determination of the profile, CFD (Computational Fluid Dynamics) analysis are carried out, to determine the response of the turbine, on all stages. All the results obtained will be used to set some boundary conditions and loads in the next optimization cycle.

- *Optimization*. This last step defines the selection of the best shapes among all studies, in other words the shapes that reflect the boundary conditions and the performance requirements are frozen and studied in depth. The geometry of the latter is studied in terms of leading and trailing edge, chordal length (i.e. axial extension of the airfoil), thickness distribution. The variations are limited to a small percentage of the basic geometry, the performance trends are tracked, and the best configuration is frozen as the Aero Pass and will be further analyzed from a mechanical point of view [8].

4.2 Preliminary Mechanical Design

Next step concerns the aerodynamic design, the phase the preliminary mechanical analysis is addressed. As first point, the profile is completed by outer and inner element. In particular, for the standard vane are used IBV (Inner Band Vane) and OBV (outer band vane), whereas to the standard blade configuration are attached dovetail (or firtree), shank and shroud. As just mentioned, these are the standard configuration nonetheless new innovative configurations are possible and currently under development.

Its important to highlight that the turbine is assembled in cold conditions in order to guarantee the right airfoil positioning in operative conditions, thus achieving the projected flowpath. This process goes through the scaling of the profile from hot to cold, being the latter determined in hot condition. The procedure followed includes:

- *Twisting*. The cross-sections projected have to twist around the radial direction in order to obtain the cold condition blade
- *Scaling*. To remove thermal expansion due to high temperature a scaling of the designed profiles is carried out
- *Positioning*. Defines the position of the elements needed to keep fixed the airfoil.

The next step regards defining a finite element model of the previously generated geometry, so as to have a complete discretization of the blade and carry out the most appropriate analysis. The main results that can be obtained at this level are: the static deformation of the system due to pressure field and the centrifugal load (in case of a rotor blade), to evaluate the mechanical stresses in steady state condition. While the forcer response will go to assess the robustness of the model. If the analysis does not produce a positive result, the profile is sent back to aerodynamic team that will tested it again through the FEM analysis.

The loop continues until satisfactory results are obtained from the FEM analysis. Considering having a positive feedback from the latest analysis, the geometry becomes definitive and the blade goes into productions. Only at this point the data obtained are processed, and in particular the Campbell diagrams are defined in order to evaluate the engine response over a wide speed range. Furthermore, flutter analysis is also performed to evaluate the possible dynamic instability due to the interaction between fluid and structure. The process according to which the further detail analysis (such as the determination of the fatigue limit) are carried out only when the geometry is already consolidated, represents one of the main problems. Therefore, following the workflow, when the results to the analysis are not satisfactory (in order to make improvement) the constraints or strengthening on blade are introduced. As a result, an increase in weight and substantial limitation to the

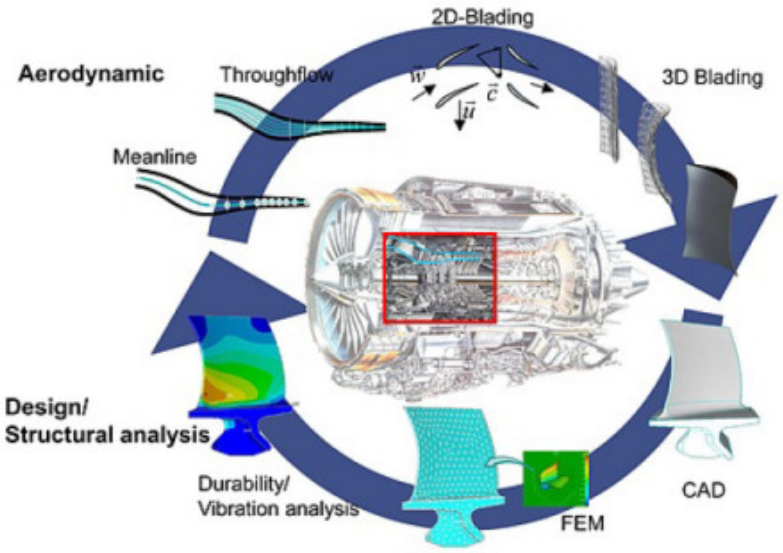

Figure 4.5: Design workflow for LP Turbine stages

aerodynamic advantages occurs. In other words, the process followed is made of two different optimization loops, one for the mechanical response and one for the aerodynamic behavior, thus not leading to a global optimum. For this reason, is therefore a need to develop a new type of design concept.

4.3 Aero-Mech Design Concept

As mentioned in the previous paragraph, to overcome the problems related to the optimization of both aerodynamic process and structural mechanics, it is necessary to introduce a new design concept. Indeed, this thesis work has as main purpose the development of an integrated model for aeromechanical design. In other words, with the introduction of *Aero-Mech design*, the possibility of inserting end elements starting from the generation of the profile has been introduced, to verify the balance and stability of the complete blade. This tool (named PRIME) is fully automated, user-friendly and with easy access and reading output. A summary of the concept discussed above, which form the core of the tool, can be observed in the figure 4.6.

PRIME (*P*reliminary ae*R*omechanics *I*ntegrated *M*ultidisciplinary *E*nvironment), aims to make the preliminary design more robust, to find the right trade-off between aerodynamic and structural requirements. In particular:

- Returns aerodynamic designers an easy to read mechanical feedback, so that they can take into account, in addition to the increase in performance, also the

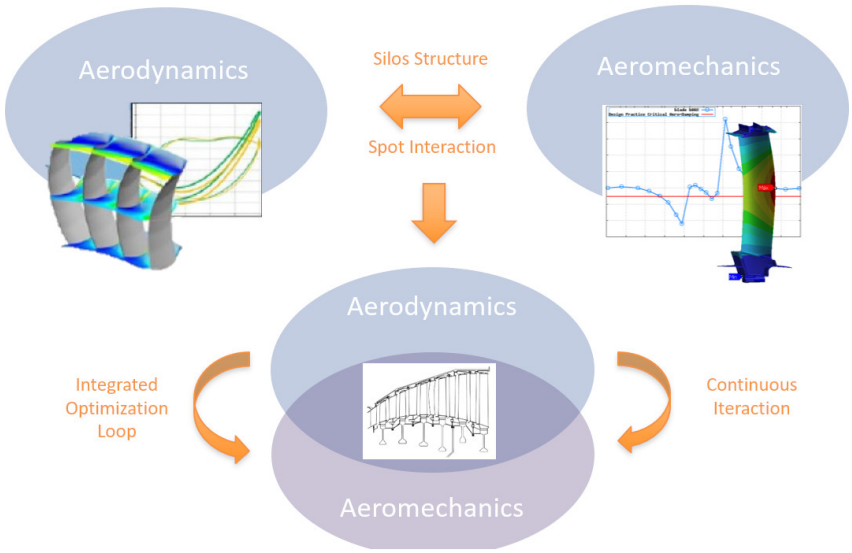

Figure 4.6: Aero-Mech design

resistance and strength of materials during the profile construction process. The tool generates a high quantity output, and for this reason the dashboard has been introduced, so that the user can interact by easily and quickly looking for the information he needs.

- The process is completely automated, as it automatically generates the CAD, the FEM model, considering the aerodynamic inputs. The automation makes the tool use-friendly, for users that dont have a deep insight in what the structural issues are and how the structural analyses are led [8].

- The user, through the tool, can receive general information on the mechanical behavior of the structure. Or he can select specific analysis, thus receiving only the information requested.

- Finally, it makes possible the definition of a global process, in order to remove time losses or/and misunderstandings in the exchange of information.

However, PRIME introduces a significant reduction in the time required to define a CAD and performs several analyses, by exploiting the potential of the Unigraphic NX and ANSYS Workbench software. With the latter software a simplified automation process and lower computation cost has been obtained (reducing the computational time), thus making it possible to introduce detailed analysis during the preliminary design. The figure 4.7, shows the underlying work flow of tool, where all routines and connections are defined. As highlighted, this thesis work focuses mainly on the CAD generation process (DynBooster), Wizard integration (the current process FEM generation build in ANSYS Workbench) and some tests

launching static analysis with subsequent generation of Campbell diagrams have been performed.

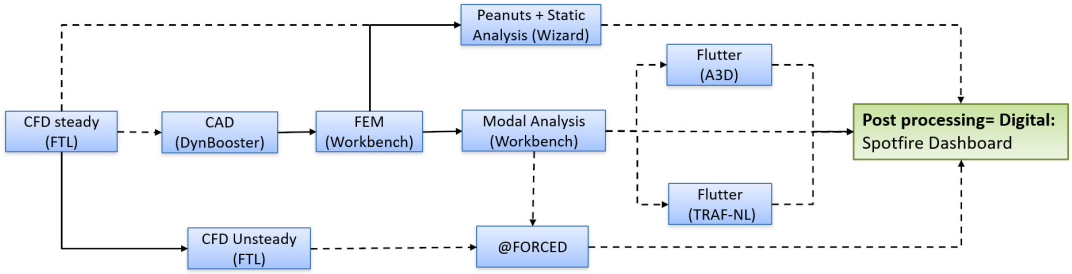

Figure 4.7: PRIME process

4.4 PRIME Process Today

Looking at figure 4.7, we can deduce that the tool can be considered as a set of connected routines, written in different programming languages. Indeed, as mentioned in the introductive chapter, this tool may be seen as a set of black-boxes bathed in a kind of glue called gateway that manages all the input and output of internal processes. The current state of the tool sees an implementation of many features, despite the frame that links all the routines has yet to be implemented. Obviously, its important to highlight that all routines defined can be runned individually. The following is a brief introduction of the functionalities development.

CAD generation. This process (dealt in-depth in chapter 5), is based on the quick generation of the complete CAD, starting from aerodynamic inputs. In particular, by inserting the aerodynamic inputs it is possible to generate the 3D airfoil and only subsequently attach the end components. The tool named DynBooster has been completed with the implementation of an interface by which the user can choose several end components, thus creating new blade configuration. Furthermore, the possibility of generating the CAD blade and disk has been implemented.

*FEM model.*This phase is subsequent to the generation of the CAD model, rather it is assumed that the CAD model has been properly generated, also considering the appropriate attribution of the tags (named selection). At this point the mesh is generated automatically as well as the loads and the boundary conditions are applied. At this level the user can choose through a simple interface with type of analysis he wants to carry out.

*Static analysis.*In this case the process starts from the definition of the loads and the boundary conditions, but before the static analysis can be performed, the peanuts plot must be defined. The latter defines the amount of interference between two adjacent blades [8] in a different operative condition of the engine. In particular the interference shall be measured as a moment or force acting on the shroud.

Modal analysis. The result of the static analysis, considering only the effect of the inertial load and temperature, is used as a pre-stress condition for the modal analysis. As output, in this case, the mode shapes and natural frequencies are defined, which are the starting point for the determination of the Campbell diagram.

Forced response. The main purpose of this analysis is the calculation of the Modal Force parameter, where through its value it is possible to understand if the structure incurs into dangerous resonance phenomena.

flutter analysis. This analysis is carried out to receive information about the aerodynamic damping, since if the latter assumes values lower than zero, the structure may incur into instability.

This process defines a simplified model suitable for preliminary analysis performing. It is also important to introduce, the possible future developments that can be implemented in PRIME. A first improvement concerns the introduction of a blade and disk analysis with appropriate conditions, considering that the CAD generation tool (DynBooster) already provides this model. A second point can be the definition of the inclusion of the tool for the High diagrams, used to analyze High Cycle Fatigue phenomena. And finally, introduce a producibility package. In this case, the plug-in mentioned would introduce the possibility to realize a CAD model which takes into account the manufacturing process capability thus making synergy between component design and production.

Chapter 5

Cad Generation Tool

As mentioned in the introductory chapter, the main purpose of this thesis work was focusing on contribution to development of a tool, called PRIME, used to carry out the preliminary design on LPT. This tool acts as a binding force between two important team cooperating in the preliminary analysis, aerodynamics and aeromechanics team, by introducing a new simulation method (Aero-Mech). The first important step to reach the goal of unifying the design both on structural and aerodynamic point of view is CAD generation. Basically, the aerodynamic team deals exclusively with the interaction between blade and fluid, carrying out the analysis based on CFD, in order to define the airfoil shape. Whereas the aeromechanic team carries out the structural analysis. To reach this goal, the aeromechanic team needs a complete cad (airfoil with extremity component) to simulate contacts correctly. The creation of complete CAD its a burdensome procedure leading to the introduction of parameterization concept.

A crucial step is to define a parametric approach in order to automatize the insertion of the templates on airfoil. This allows to modify the shapes of the templates depending on the aerodynamic input and speeds up the entire procedure. The template generation starts from cross-section in order to create a realistic template and continues with the definition of a set of parameters appropriately grouped. All kind of templates generated follow a parametric approach and a robust logic so as to simplify the process creation and substantially reduce the used parameters. The parameters are assembled in three different groups: system, coupled and custom parameters. To complete the groups there is general information where the global template knowledge is contained. The whole process is managed by a tool called DynBooster, the tool subject of this work.

As it will be set out in the following paragraphs, the majority of DynBooster code has been rewritten in Matlab, with a flexible and robust logic, thereby facilitating the accessibility and integration in the Wizard process (the process FEM generation build in ANSYS Workbench). Furthermore, the improvement, replacement therefore the creations of new code parts have been implemented, in addition

to considering a new logic to create more realistic parametric templates. In conclusion, a GUI has been redefined in order to generate new CAD configuration,and also a procedure for calculating a perfect blade stacking has been integrated. The disk has been inserted in order to realize bladed disk CAD and also converter for CAD templates has been added. All those above mentioned operations will be in-depth analyzed later.

5.1 DynBooster

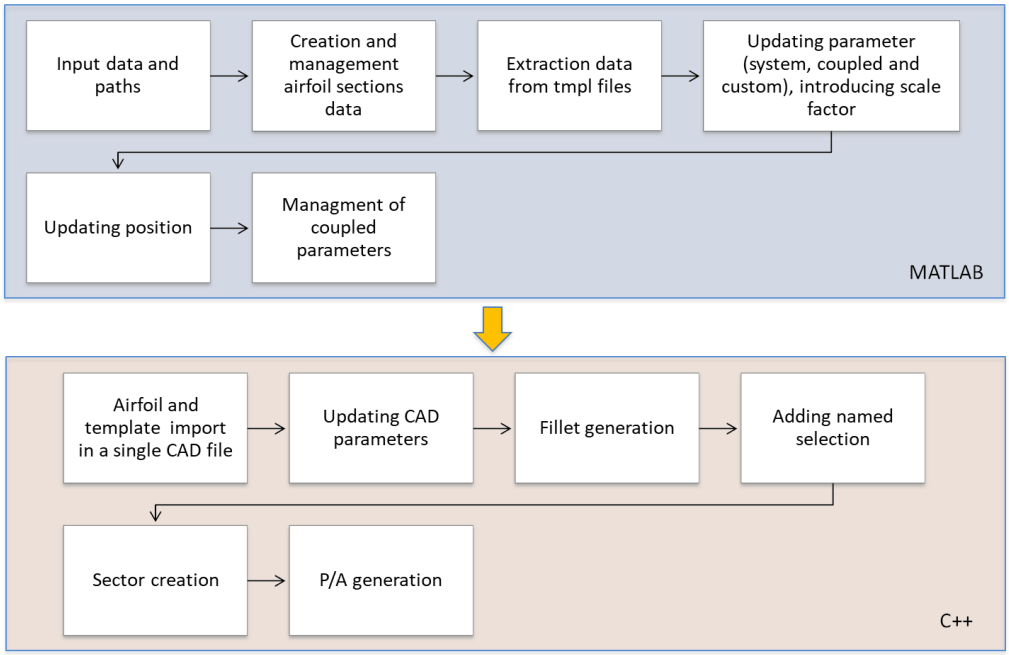

Figure 5.1: DynBooster workflow both matlab and C++ side

As in the previous paragraph mentioned briefly, the tool that handles the CAD generation process is named DynBooster. The main part of this thesis work focused on a substantial modification of DynBooster code, rewritten for most in Matlab. Basically, the tool involves two parts:

- The Matlab part, that manages the reading and writing process of template parameters, in addition to definition of the right value of all important parameters used for the positioning and centering.
- The C++ part, which constitutes the tool core. This part has been written with this language because it must be able to interface with Unigraphics NX (work environment used for the creation of parametric templates). In other

words, in this case its possible to update all the parameters as far as generate the connection element (fillet).

In particular, the workflow of DynBooster code includes in the first step some general information as name of template and important folders paths. Subsequently, it deals with the definition of the parameters used for the creation of airfoil, in addition it manages the extraction of templates parameters from *tmpl* files (one of the core files used in templating and contains the parameters groups specified previously: system, custom, coupled and general information group). In the next step all the parameters are adapted based on the inserted aerodynamic input, as well as the position and the scale factor are defined. An important point, analyzed later, is defined by identification of the coupled parameters, in order to have an optimal positioning and centering of the airfoil templates.

In DynBooster core part a process of operations are performed interfacing with NX. As first step the Cad airfoil part is generated, as well as the parameters of templates are updated. The assembly of all components, considering also the generation of fillets and named selection, play a basic role. This last operation concerns in adding tags where the loads, constraints or specific mesh requests are applied, and then be recognized and used in Ansys Workbench analysis FEM. At the end the code includes the union of the body, the creation of sectors with a several numbers of airfoil and the generation of P/A files. It is a file used to calculate the P/A value, through the ratio between centrifugal force and plan section of the blade evaluated at different distances from the engine axis.

The Dynbooster code was conceived to manage two different working modes: default and custom mode. In the default mode, the CAD is generated quickly with an automatized procedure where its possible to choose the desired cad type (vane, blade only, bladed disk and new configuration type) and the number of stage and sectors. While the custom mode is composed by a GUI (graphical user interfaces) that allows to customize all template parameters and create innovative blade configurations.

5.2 Airfoil Creation

The airfoil creation defines the first important step for the CAD generation. The procedure followed, as defined previously, can be divided in two parts: the acquisition and writing part and the creation part of airfoil CAD. The first part is handled in Matlab and concerns the reading of 2D profile aerodynamics data at hub and tip of blade. These data are saved in a standardised file and play the main role in the connection of the various templates with airfoil. The accessibility of the aerodynamics data allows the continuous updating of the parameters template, through a set of sizes calculated by tool. If the airfoil is already available, the tool is limited to import it in the work environment.

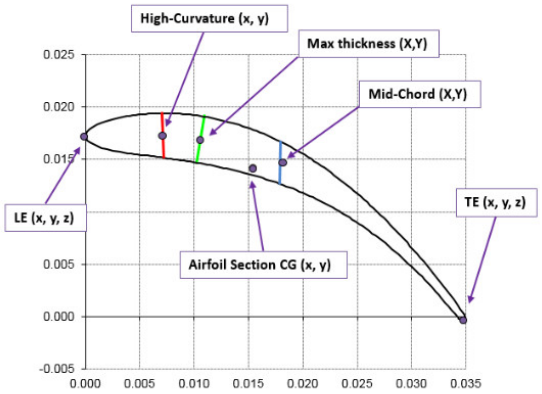

Figure 5.2: 2D airfoil section

The creation part of 3D airfoil is defined in DynBooster core, considering the previous structure aerodynamics data. The airfoil generation, as shown in a figure 5.3 (b), starts from splines creation and through a process of creation and union of surfaces realizes the cad part. The named selection, in this case, is arranged to the faces shown in a figure 5.3 (a), in order to differentiate the leading edge, trailing edge, pressure and suction side used for FEM analysis.

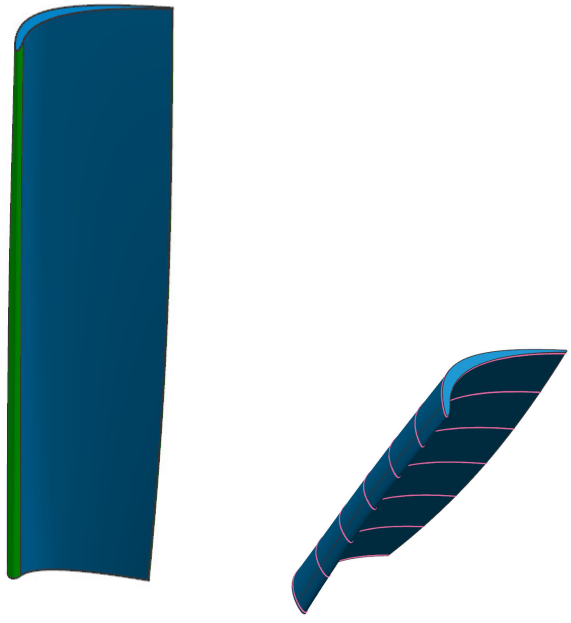

(a) Airfoil view 1 (b) Airfoil view 2

Figure 5.3: 3D Airfoil produced by DynBooster

5.3 Logic Process for the Definition of Parametric Templates

Once completed the process of generating the airfoil part, it is necessary to define the extremity components in order to have the whole CAD used for the FEM analysis. For this purpose, several parametric templates have been built and inserted in the tool database, thus allowing the user to generate different configurations and types of blade. From this point of view, the code has been created considering the possibility for the user to insert a new type of template. This has been made possible based on generating structures that can be updated continuously. One of the main points, which will be developed in the following paragraph, concerns the new developed strategy for the templates creation. The latter introduces several improvements to previous strategy, as:

- Simplification of the process to create parametric templates, aiming to generate it with a few and simple steps.
- Improvements of the parametric templates geometry.
- Reduction of custom parameters.
- Robust logic of the creation process, namely the reduction of possible failure during the parameters updating.

As a result of these improvements, may be taken into account: more realistic parametric templates, the number reduction of parameters that the code manages and the creation time reduction.

In other words, this process defines the complete parametrization of the templates, allowing the shape modification with the simple parameters change. As it was introduced in a previous paragraph, the parameters are divided in three groups:

- System parameters, automatically updated and able to allow the connection between blade and templates. These parameters are extracted from 2D airfoil data at hub and tip. The most considerable are: the inclination at the end of airfoil, the minimal chordal length and the reference radius from engine axis.
- Custom parameters are completely customized by user and they are further divided in: lengths, thicknesses, fillets radius and angles. Consequently, the parameters updating the size and shape of the templates change.
- Coupled parameters are common data sets between two templates and they are used to realize optimal positioning and assembly.

All the parameters identified, before being customized by the user, are appropriately scaled and manipulated based on aerodynamics input. Manipulation means the variation of the key parameters (as cut angles), which may change because of aerodynamics input variation (for instance, when the stagger or the exit angle change, figure 5.4).

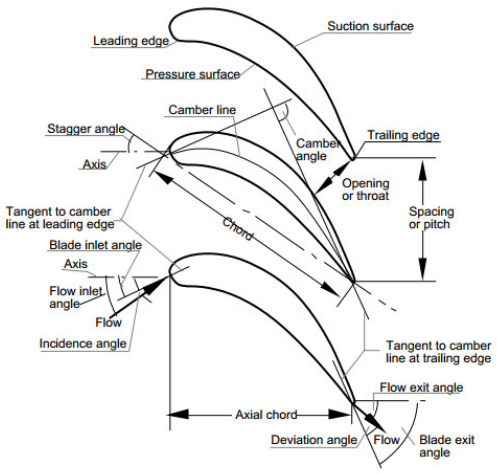

Figure 5.4: Blade Nomenclature

The parametric templates have been generated considering the engine cross-section as reference. In particular, the extremity component of blade, vane and other innovative templates have been created. The procedure followed, starting from 2D sketch creation (as shown in a figure 5.5-b) and throughout the revolution of the latter about the engine axis, allows to generate the 3D component. The revolved shape is then trimmed with surfaces generated through concatenation of planes, each of them aligned to a specific angle (cut angle) determined by the local shape of the airfoil. Other templates will be shown in the 5.4 paragraph.

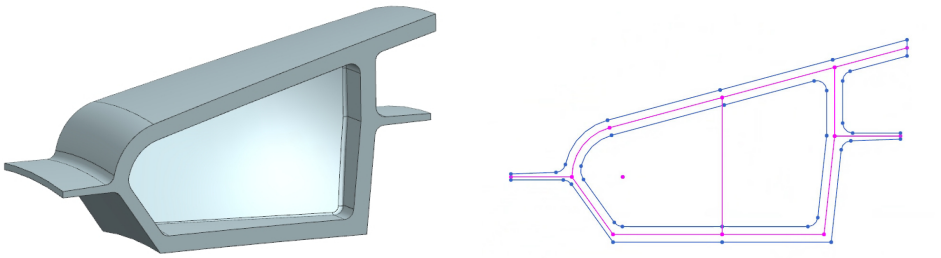

(a) Shank template (b) Sketch of Shank configuration

Figure 5.5: New Shank configuration

Finally, this new way of conceiving the development of a parametric template, as already mentioned, leads to the generation of more realistic components, making it possible to create complex shapes as shown in figure 5.6(a). In this specific case (figure 5.7), some body subtraction techniques are used to reduce the component mass.

5.4 Centering and Assembly of Templates

The positioning and centering of the templates are the most important steps in the assembly of the whole CAD. In the following paragraph, technique used to

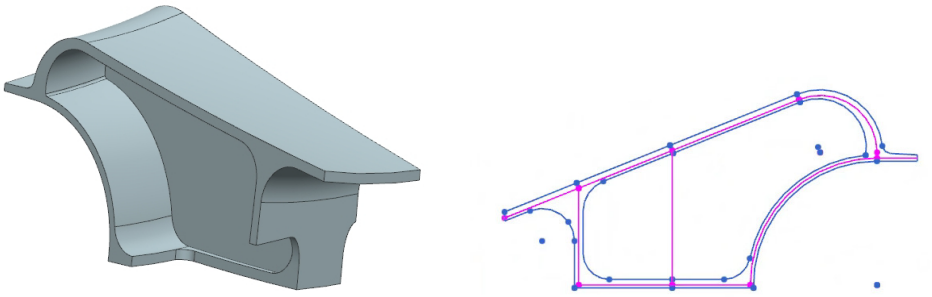

(a) Shank template (b) Sketch of shank configuration

Figure 5.6: New Shank with a mass reduction

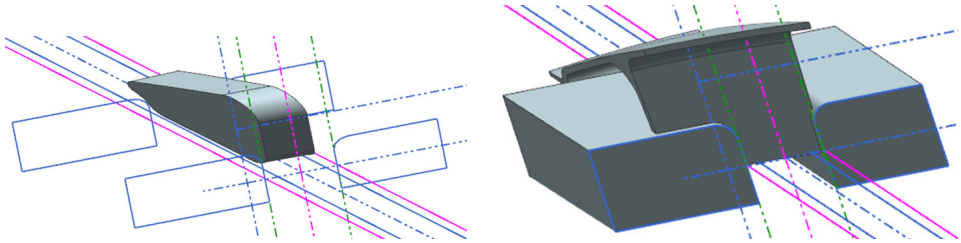

(a) Introducing of the side section (b) Body subtraction techniques

Figure 5.7: New strategy for component mass reduction

perfectly balance the blade is described.As first step, the airfoil and all the templates required to generate the blade model are imported in the same CAD part and the latter are centered with respect to the center of gravity of the closest airfoil section. This involves the definition of an axial and tangential offset, determined from four main point: leading edge, trailing edge, max curvature and max thickness [19]. Its important to consider further the determination of cut angles, that play a main role in the perfect templates positioning. The calculation of these system parameters is strongly dependent on the kind of template considered: the following paragraph will introduce the logics beyond main parameter setting.

5.4.1 Shroud Modeling

As shown in a figure 5.8 the Shroud templates is defined through several cut angles (such as interlock angle) that change depending on aerodynamic input.In this case, the interlocking is positioned in correspondence to the airfoil section maximum thickness. Indeed, the sketch has been realized so that the dimension (height and width) and the angle of the interlock, don't change when the parameters are updated by the software. These quantities are defined as hybrid parameters and can be edited from user.In order to balance the tip shroud bending moment about

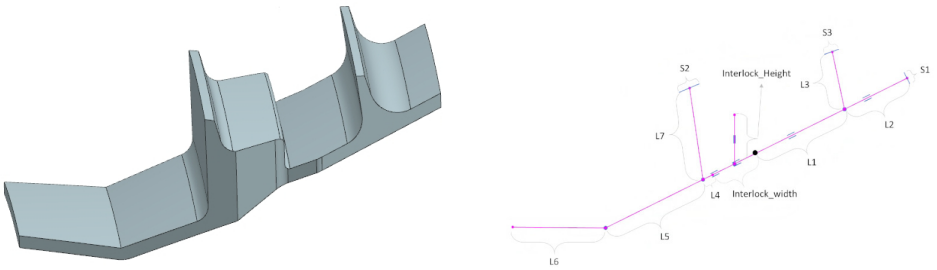

(a) shroud template (b) Sketch of Shroud configuration

Figure 5.8: Shroud, sketch and template

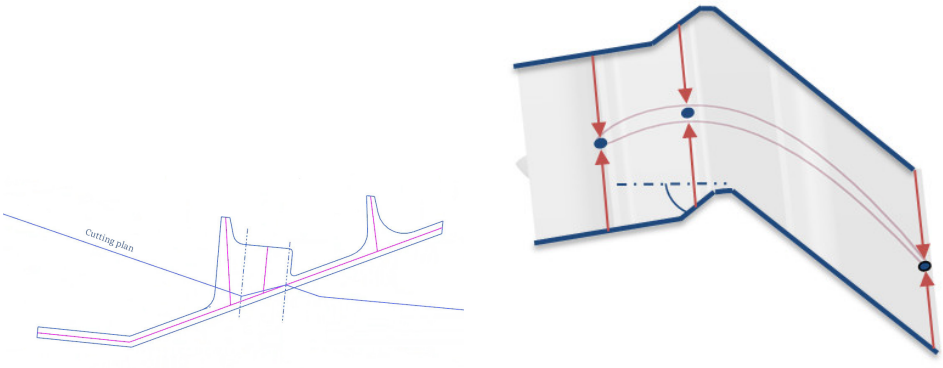

(a) Shroud cutting plan (b) Three point centering strategy

Figure 5.9: Drawing details Shroud configuration

the airfoil tip section, a three point centering strategy has been adopted: airfoil LE (leading edge), TE (trailing edge) and maximum thickness points (see figure5.9-b) will be each at equal distance to the bounding planes.

5.4.2 Shank Modeling

The shank modeling, starts from 2D sketch drawing (figures 5.10-b,d) considering the real dimension defined from engine cross-section. This sketch is parameterized and as it will be defined later, it is constituted by coupled parameters that allow a perfect matching between the parts.

In particular, in this case the 3D template is defined through a body trim, considering only one cutting angle. As shown in a figure 5.11 it has been followed a new strategy to center the blade in a single cut angle case. This strategy is based on the following actions:

- Extracting points from aerodynamic input, in order to define the shape of the

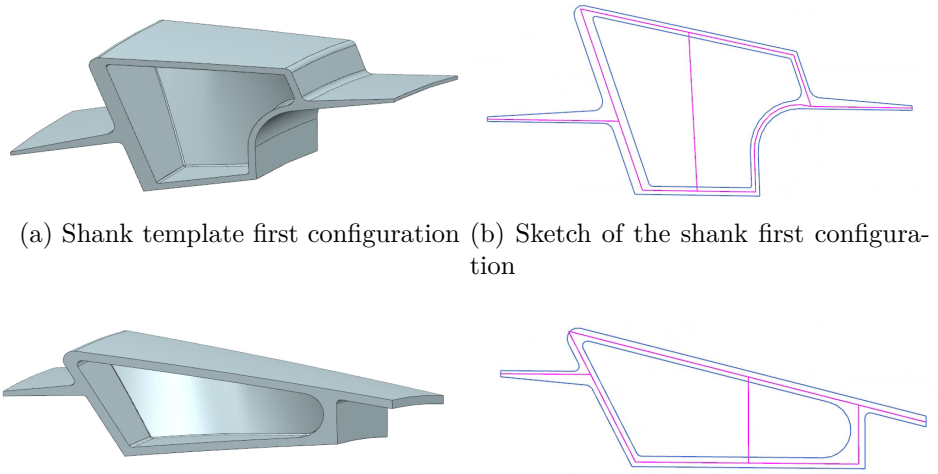

(a) Shank template first configuration (b) Sketch of the shank first configuration

(c) shank template second configuration (d) Sketch of the shank second configuration

Figure 5.10: Shank templates

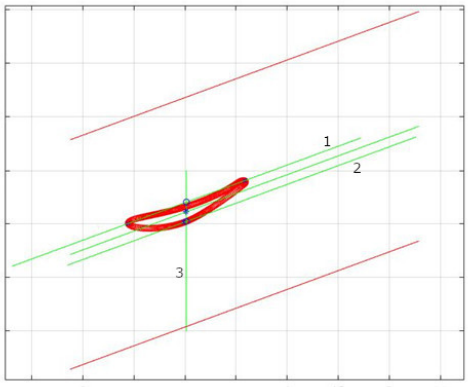

Figure 5.11: Blade centering techniques with a single cut angle

airfoil section (figure 5.11-a)

- Drawing the chord between LE (leading edge) and TE (trailing edge), as shown in figure 5.11-a (line 1)
- Outlining the parallel on the SS (suction side), passing through the max thickness (line 2, figure 5.11-a)
- Drawing the central axis and find the intersection points with other lines (line 3, figure 5.11-a)
- Finally, determining the centerline point, we are able to define the tangential

offset to have a perfect centering on the platform shank.

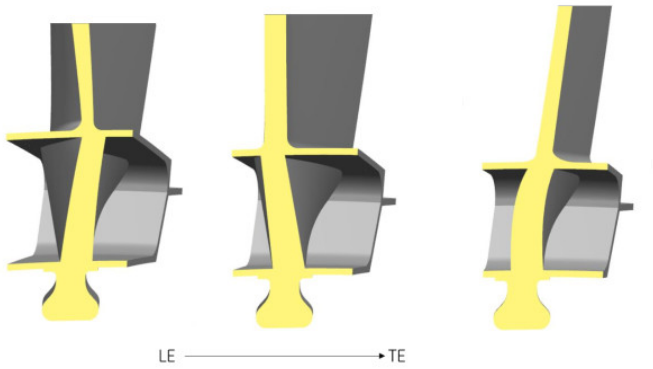

Figure 5.12: Sections of shank inner pocket

In contrast to the shroud, the shank template has been modelled, following a simple step, since the only design rule is to accept that the single cutting and stagger angle are equal. In general, the shank is divided into two sub-components, the external one and the inner pocket. The latter performs the function of supporting the airfoil and allows the connection between dovetail and blade. The pocket definition (figure 5.12), is based on a four points centering strategy (middle point, max thickness, leading edge and trailing edge), in order to follow the profile of the hub airfoil section in the upper part and the geometry of the dovetail on the lower part (figure 5.13-b).

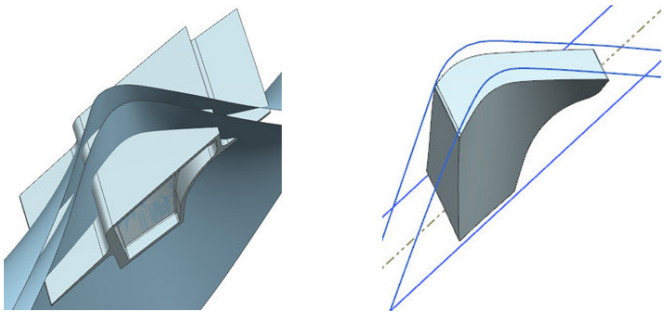

(a) Shroud cutting plan

(b) Three point centering strategy

Figure 5.13: Drawing details Shroud configuration

5.4.3 Dovetail Modeling

To complete the blade only configuration, the dovetail modeling is shown below. In the preliminary phase, the engine cross-section has been taken as reference for the dovetail modeling. As a result, the process followed is the same described in the previous cases, with an only difference that regards the groups of parameters. In this case there are only coupled and system parameters, because:

- The shape of the this templates will be manipulated by a dedicated plug-in which is going to be integrated in DynBooster in a future work. That is why the names of coupled parameters are same to those laid down in the plug-in.

- All the parameters cant be customized, as they are common parameters between Dovetail and disk and for this defined as coupled parameters.

It has been modelled two types of Dovetail (figure 5.14), that differ in number of lobes, paying particular attention to contact areas.

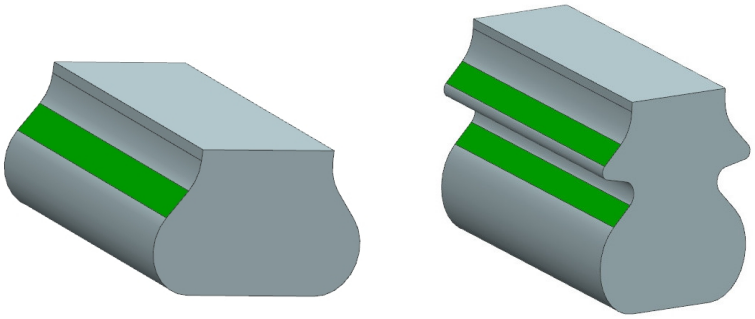

Figure 5.14: Dovetail templates

5.5 Coupled Parameters

In the previous paragraph it has been in depth described the positioning and centering of the template at tip and hub of the blade. Also, for the inner and outer templates of vane, the same procedure is followed for both design rule and positioning. In the blade only configuration, the parameters that define a right match between the parts, have an essential role. Therefore, a new logic to manage the coupled parameters have been introduced.

Underlying of this procedure, there is the concept based on the split of two different coupled parameters:

- *Master* coupled parameters, contains the group of parameters that define the shape of the geometry as shown in a figure 5.15. In this case (Dovetail templates), the master coupled parameters are composed of: dovetail extension, *Dovetail-Extension*, *Dovetail-A-shank* and *Dovetail-drif-angle*.
- *Slave* coupled parameters, is the group of parameters modified according to the master coupled parameters, in order to have a perdect matching. Indeed, observing figure 5.16, the two parameters named *Dovetail-Extension* master and *Dovetail-Extension* slave must be identical when the loop associated with the update of the coupled parameters is completed.

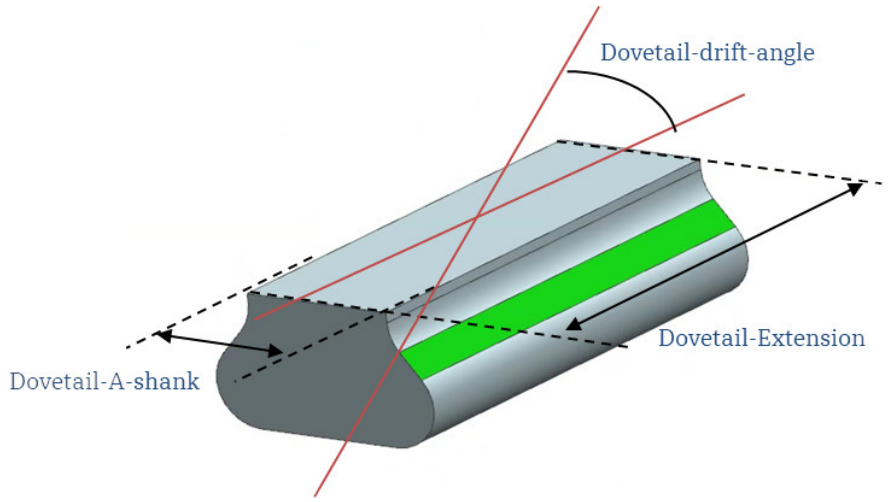

Figure 5.15: Master - Coupled parameters

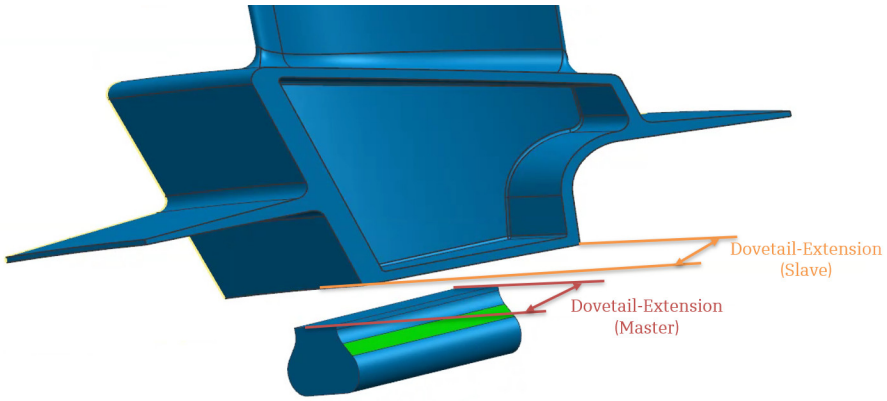

Figure 5.16: Master and Slave - Coupled parameters

Another aspect which should be highlighted concerns the process followed for data updating. The code has been set so that the name given to the parameters

identifies the master or slave coupled parameters. Only after identification, all other parameters (slave coupled parameters) take the same value. In the figure 5.17, we can observe the results obtained.

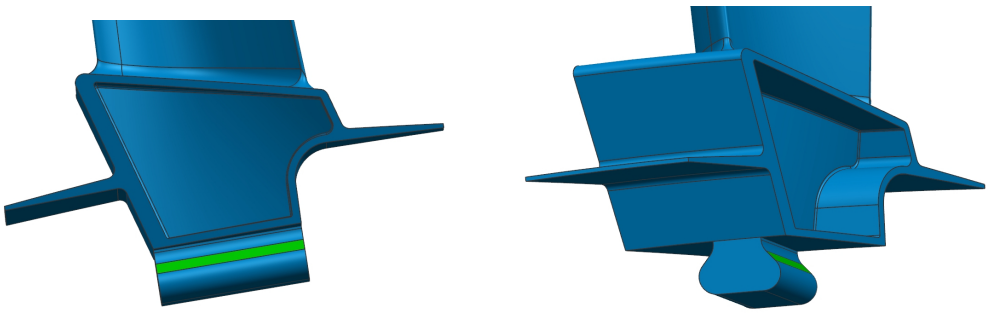

(a) view 1 (b) view 2

Figure 5.17: Dovetail - shank matching

5.6 Blade Only and Vane Configuration

Two important topics have been previously described:

- The logic of the template creation process that led to the determination of several blade configuration.
- The automatic update data so that the extremity component can comply with to different aerodynamics input. This allows the right positioning and centering.

The next step is to assembly all the components, considering also the match between shank and dovetail (coupled parameters) explained in 5.5 paragraph. This procedure takes place in the Unigraphic NX environments through a part of code written in C++. The implemented routine works as follows:

- Importing airfoil and templates as separated bodies in a single CAD file.
- Updating all the parameters associated with the templates upon the current airfoil characteristics
- Linking the bodies with boolean union operation (e.g. between shank and dovetail templates) or by creating a fillet (e.g. between tip shroud template and airfoil)
- Adding tags (Named Selections) and properties to key features to interface the model with Ansys Workbench (see paragraph 6.1)

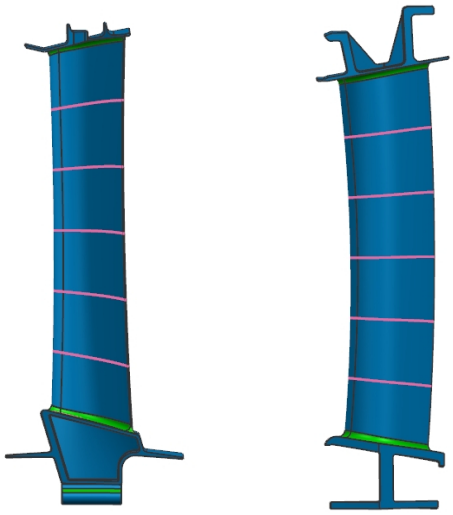

(a) Blade (b) Vane

Figure 5.18: Blade only and vane configuration

It deserves to mention that a robust iterative procedure has been implemented to create the fillets between the airfoil and the templates interfacing with it.

In figure 5.18 (b) the vane is composed by two end components: IBV (inner band vane) and OBV (outer band vane). The following details deserve to be defined:

- For the IBV two templates have been generated that differ in the introduction of the interlock (see figure 5.19-a)

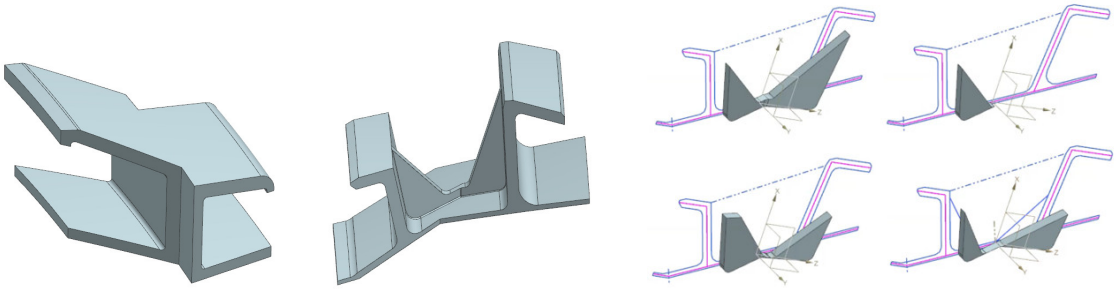

(a) Inner Band Vane with interlock (b) Outer Band Vane (c) OBV: Gasset configuration

Figure 5.19: Vane end components

- The OBV was introduced considering a new strategy to manage the gasset. In this case four different possible configurations have been implemented as shown in the figure 5.19 (c).

5.7 Sector Generation

An important option provided by DynBooster code, is to define the size segments for the selected model (figure 5.20). The procedure implemented is based on the following steps:

- CAD generation, following all the operations defined in paragraph 5.6.
- Copying and rotating the bodies considering the angle defined as: (stage airfoil count)/360

Finally, the user with this method could perform a study on whole ring blade (figure 5.20-c).

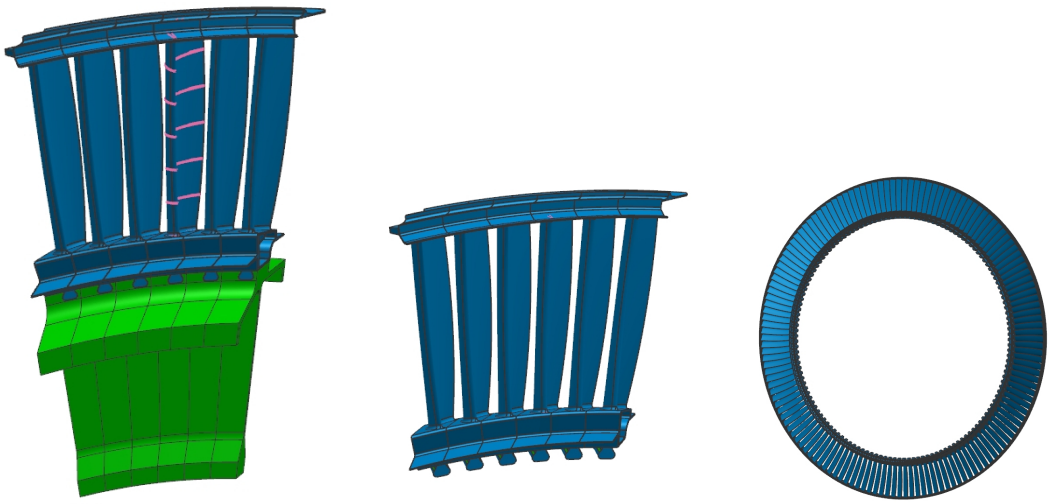

(a) Sector Blade/disk (b) Sector Blade only (c) The whole ring blade

Figure 5.20: Examples of Sectors

5.8 Blade/disk configuration

In addition to blade only and vane configuration, blade/disk has been implemented. The workflow considered for CAD generation is based on procedure introduced in paragraph 5.3. Two main steps should be highlighted in this case:

- Intersection of bodies (dovetail and disk) with boolean subtraction operation.
- In order to have a correct matching between the bodies, all the parameters that define the dovetail shape (figure 5.21) are added in the coupled parameters group. At this point, it is possible to follow the same procedure described in paragraph 5.5

Nevertheless, the process followed for the definition of dovetail starts from generation of 2D sketch, considering the engine cross-section as reference. The next step is the extrusion of dovetail sketch, and subtract it from the disk. An important step is based on the definition of cut angles, used to trim the body. In this case the coupled parameters have been introduced between shank and disk, so that the respective cutting angles are equal.Through this procedure, we can obtain a different drift of dovetail respect to the cutting plane (figure 5.22-b)

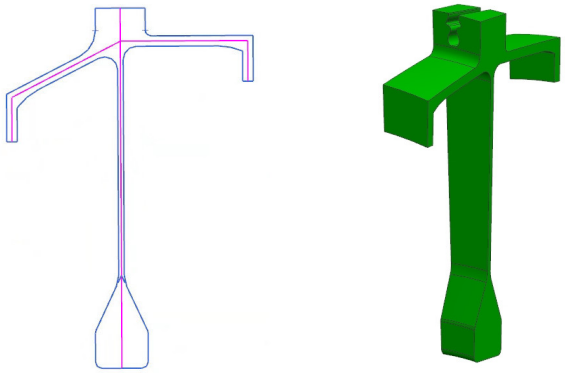

(a) Sketch of Disk configuration (b) Disk template

Figure 5.21: Disk, sketch and template

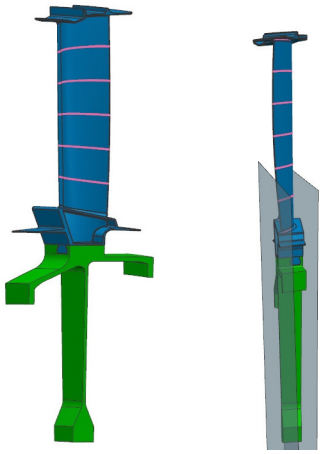

(a) Blade/Disk (b) Disk cutting plane

Figure 5.22: Blade/Disk CAD

Chapter 6

Wizard Integration and FEM Analysis

Before introducing the topics concerning the integration of DynBooster in Wizard and the GUI for the generation of new blade configuration, its necessary to define the Wizard part. When DynBooster process is finished, a CAD is defined with appropriate tags (named selection). The next step is to perform the FEM analysis, starting from mesh generation with subsequent application of loads and boundary conditions. In particular the centrifugal load and a 2D thermal load (in form of a 2D temperature map) will be applied. In the preliminary design phase, the whole procedure is automatized through the Wizard generation that works in Ansys Workbench environment.

6.1 DynBooster Integration and Named Selection

One of the first step performed in the Wizard workflow is the part concerned Cad generation. Therefore, it plays a main role the integration of executable Dynbooster in wizard. This process takes place by file input creation that DynBooster reads automatically. The latter is composed of several inputs:

- The name of model that matches the name of Workbench project
- The type of model considered (for instance blade, vane or other models)
- Unit of measurement (Imperial or Metric)
- The working mode of DynBooster tool (custom or default mode)
- The path of different folders relevant to tool functioning

Nevertheless, this input file is generated by Wizard through information inserted by the user (figure 6.1). To make the tool user friendly, a graphic interface has been created where the user can choose the analysis to be performed and introduce the inputs.

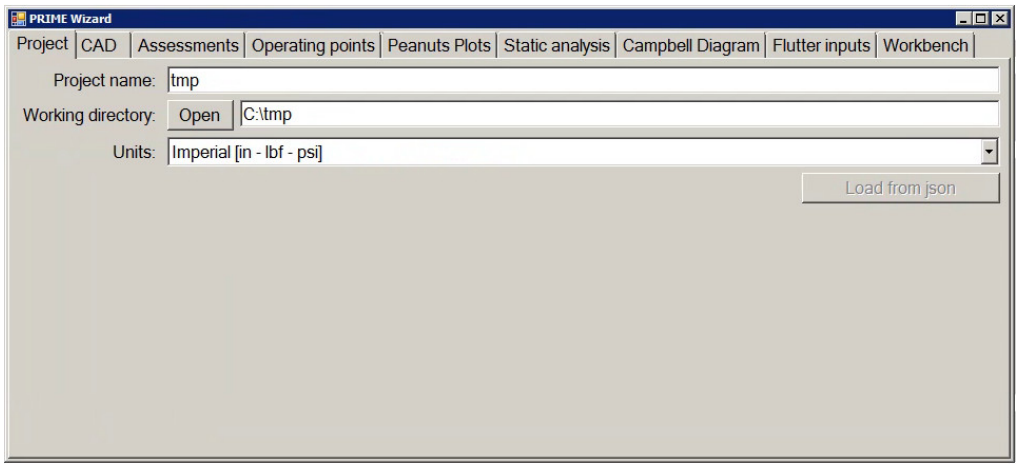

Figure 6.1: PRIME graphic interface

As shown in a figure 6.1, the tool interface is divided in different tabs where the user can insert:

- The input for Cad generation (As described previously)
- The type of assessments: Peanuts plots, static analysis, campbell diagram and flutter inputs. These have been described in . paragraph

At this point, its necessary to introduce in-depth the tool workflow, considering the CAD has already been treated. As first step, reading of named selection is performed in order to give correct constrain and boundary conditions (figure 6.2).

In Workbench environment, the mesh is automatically generated also on contact faces where perfect match is required. As described in the first part, the thermal load is inserted in form of 2D temperature map (function of radial and tangential coordinates). As a result, the thermal map will be generated which determines the different local use value, related to the material tensile modulus. Subsequently the solution is calculated through:

- Static analysis performed considering all load cases and boundary conditions. Nevertheless, before this analysis is carried out, the peanuts plots must be defined.The "peanuts plots" are line charts representing the change of interlocking behaviour (in terms of force and interference) during engine off-design conditions.

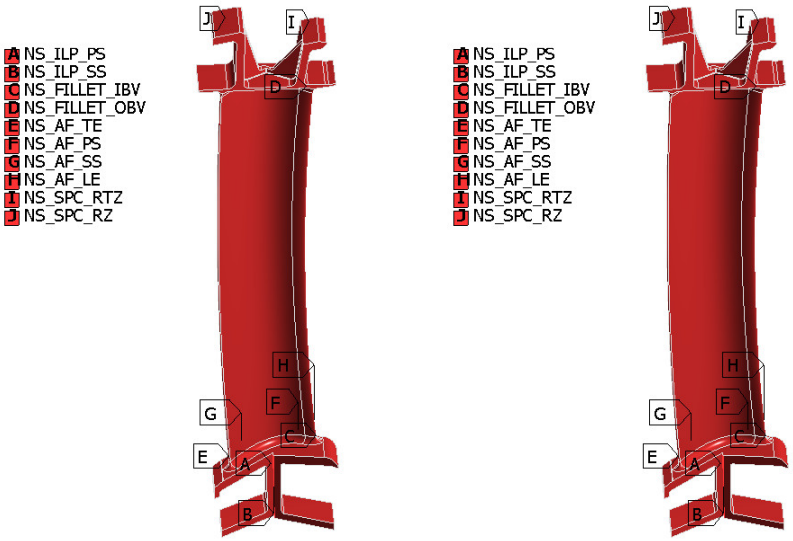

(a) Vane named selection (b) Blade named selection

Figure 6.2: Named Selection

- Modal analysis is defined on the basis of pre-stress condition. The latter is due to the static analysis performed considering the temperature effects and inertial load. As output the modeshapes and natural frequencies are defined, in addition to the report generation for the subsequent forced response and flutter analysis (not yet integrated in PRIME package). Finally, the main output of the free response calculation is the Campbell diagram

In the post processing all the output data will be read by a dashboard that shows several information from the analysis.

6.2 DynBooster GUI for New Innovative LPT Geometry

As already mentioned in a previous chapter, DynBooster tool can work with two modes: default and custom. In particular, being the studies of new innovative engines still go through a learning phase, various options about structure of blade are weighted up. Therefore, it has been ever-increasing the necessity to implement a loop able to define new configuration of blades. This consequently gives rise the DynBooster custom version where the code has been completely rewritten in order to manage all the templates and new working modes described in-depth in the previous chapter. To make the whole thing use-friendly, it has been inserted a new

Graphical User Interface (GUI) where the user can create about 96 configurations of blades as well as editing all custom parameters for each template. The default working mode instead, relies on some pre-determined combinations of templates and gives no customization possibility of any of them to the user.

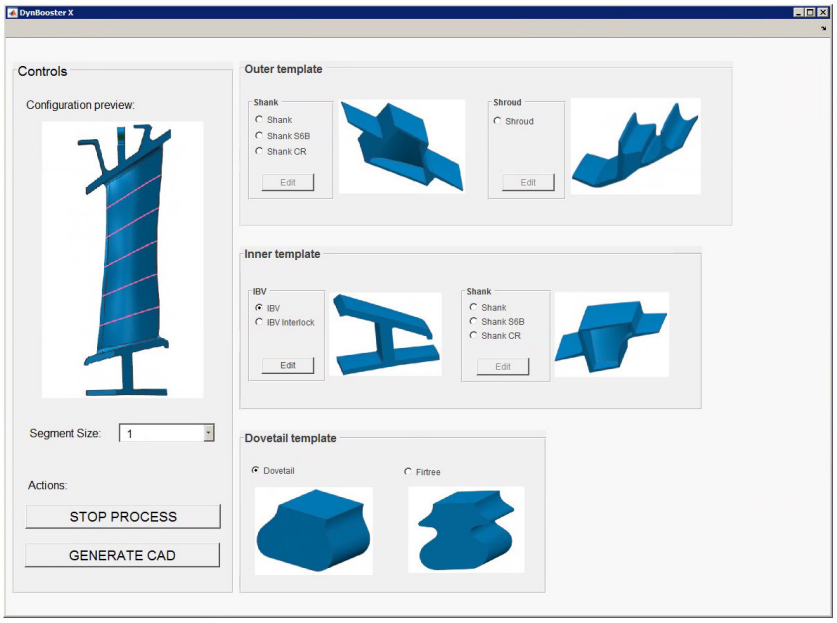

Figure 6.3: DynBooster, Graphical User Interface (GUI)

As shown in a figure 6.3 the GUI for the custom working mode is very intuitive, and it has been programmed to avoid the selection of templates that cannot be matched. Despite the different aerodynamical file inserted (AF), through this GUI the user can generate with an automatic procedure, an innovative CAD subsequently introduced in Wizard for FEM analysis. These steps allow to analyze in a short time with an instant feedback on configuration and significant time and resources saving. Moreover, the user through the edit button, can access to another interface where its possible to modify all the custom parameters defined in the templates (figure 6.4). This has been made possible by parametrization of the template extensively explained in the 5.3 paragraph.

One of the key points in the writing of DynBooster custom version has been the management of multiple templates of the same type. In particular, as can be seen in the figure 6.3, for OBV, IBV and Shank are defined different type of templates. This led to development of a structure able to manage more templates for each type. What is more, thanks to this structure, any new template that will be added to the database, requires no modification to the code in order to make it available for the selection. Finally, in the next figure 6.5, different new configurations of blade, vane and blade/disk are showed.

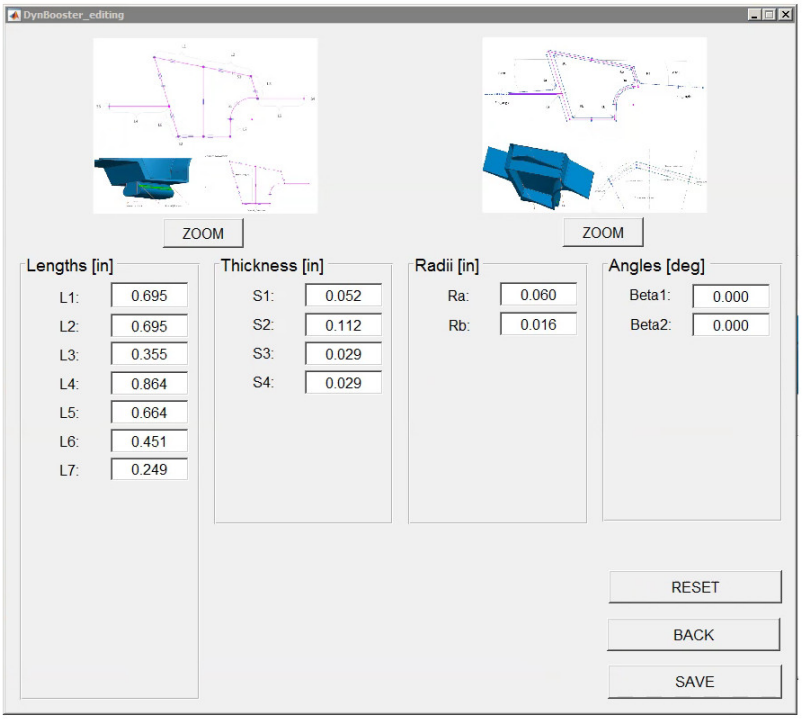

Figure 6.4: Customizing template through graphic interface

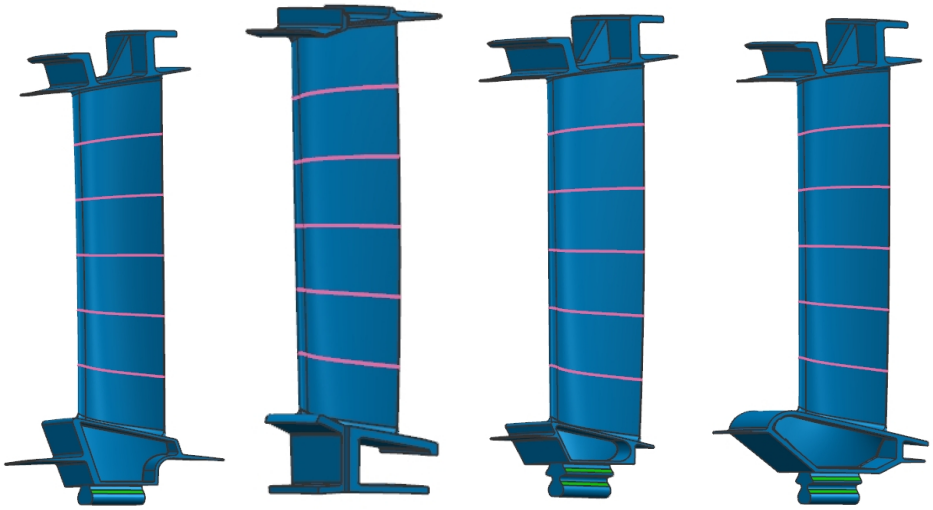

Figure 6.5: New blade configurations

6.3 PRIME - Test Case

After the whole package of DynBooster tool is integrated in Wizard, it has been possible to carry out different kind of analysis (through PRIME tool). In particular the following analysis have been performed:

- Static analysis with subsequent generation of Campbell diagrams. In this cases, different types of airfoil has been analyzed in order to match the result. Furthermore, the validation between Nastran Workbench (work environment of Wizard) has been defined.
- Considering new configuration blade, the effect of airfoil count per segment on system and profile modes has been evaluated.

6.3.1 Static Analysis and Campbell Diagram

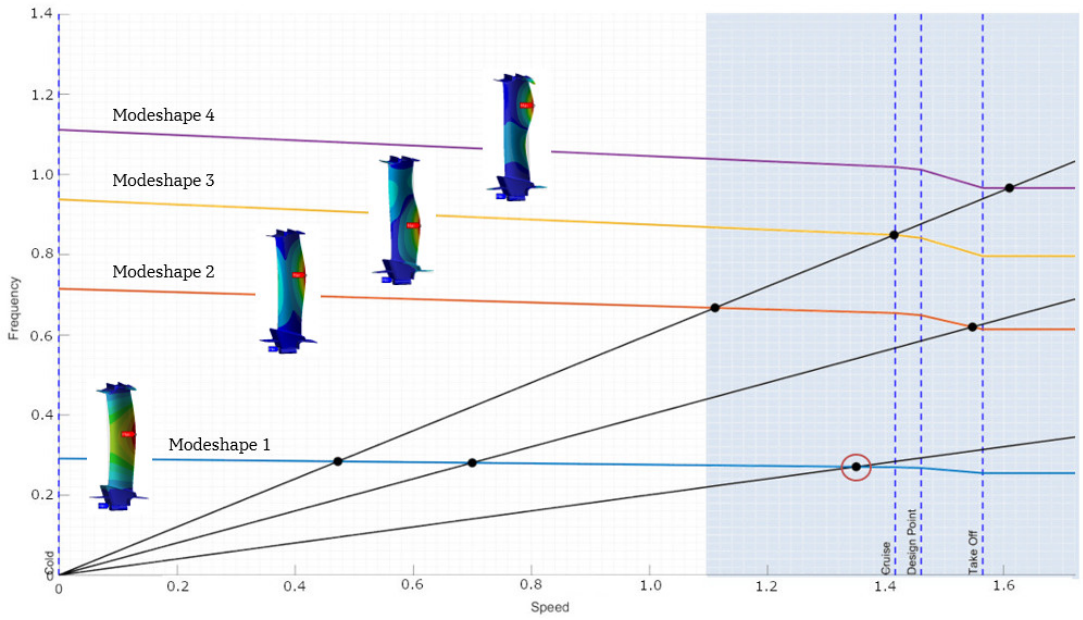

Figure 6.6: Campbell diagram and modeshapes

For this type of analysis, it has been considered a preliminary geometry for shank, shroud and dovetail (produced by DynBooster). The analysis has been performed on first stage of a new configuration turbine, considering two types of airfoil with different geometry characteristics. In this case the dof grounded has been inserted on dovetail contact face, while the constrain on interlocking face is radial free. Therefore, its extremely important to have identical meshes on interlock both pressure and suction side.

The operative condition inserted are cold, cruise, design point and take off, where for each one of these, temperature maps and rotational speed have been introduced. In particular, being a new configuration of turbine the constant temperature maps for cruise and take-off are introduced, whereas a temperature 1D spanwise is inserted for the design point condition. The first examined step concerns the comparison between two different airfoils, based on the analyzes carried out. Despite, after the choice of the airfoil, the main purpose at this point is to define the modalshapes and relative frequency for all operative conditions, in order to generate the Campbell diagram and identify the potentially dangerous crossing. In the following figure 6.6, is showed an example of modeshapes determined, and the subsequently Campbell diagram.

Through the Campbell diagram, considering a operative range increase, it has been possible to identify the potentially dangerous crossing with 1F shall be moved away from operating range.

6.3.2 Effect of Airfoil Count per Segment

In this kind of analysis, the main goal was to study the effect of airfoil count on the frequency and modeshapes. Through DynBooster, the several segments have been generated, considering the choice of the following template: IBV (inner band vane) with interlocking and OBV (outer band Vane). In the figure 6.7, is shown a classification of constrains, where the SPC (Single Point Constrain) in radial, tangential and axial direction is applied on hook. This means that the nodes displacements are set to zero in all three directions. Whereas the free condition (where the blade is free to vibrate) is applied on IBV with interlocking. After this step, through the use of Prime and introducing the operative conditions, material and temperature maps, the analysis have been possible. By setting correctly all these steps, we have come to determination of different modeshapes.

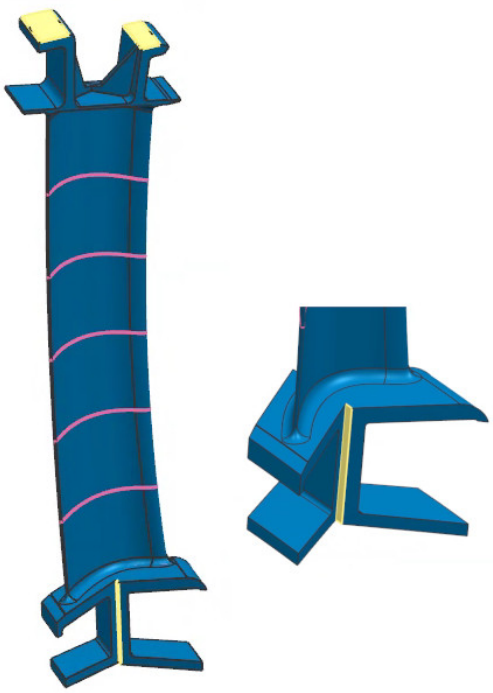

Figure 6.7: Position of the constraints

The first modeshapes distinction is the subdivision into blade modes and system modes. The system mode takes place at low natural frequencies and can be classified as flap, twist and edgewise modes (figure 6.8). The flap case occurs a low dependence

from constrain interlock and introduce a displacement perpendicular to the blade chord. Whereas in the edgewise mode the platform moves in axial direction, showing an high interlock dependence.

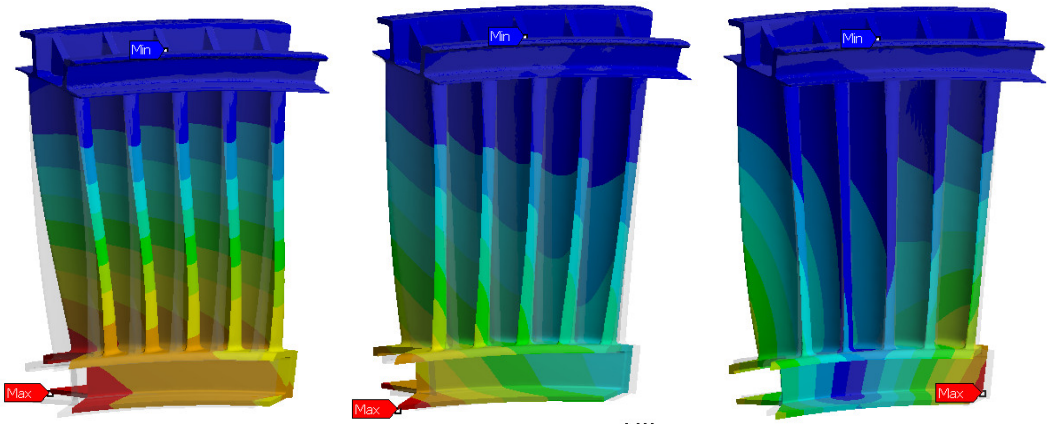

Figure 6.8: System modes: Flap, Twist and Edgewise

In the profile modes, the deformation is focused more on the profile, indeed the casing and the platform remain unchanged. In this case, flectional and torsional mode define the principal modeshapes and the latter are showed in a following figure 6.9.

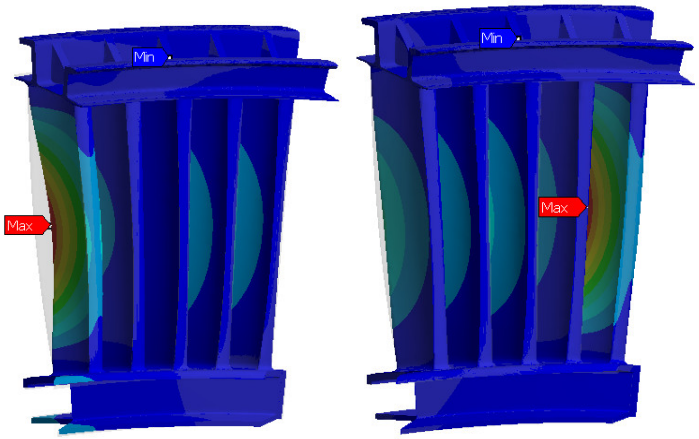

Figure 6.9: Blade modes: flectional and torsional

The main point of this study is defined by the diagram in the figure 6.10 where considering the system modes, we focus on the trend of frequency when the number of airfoil change. The results obtained show an increase of frequency from single

airfoil analysis to segment with two airfoils and a subsequent stabilization of the frequencies.This is due to the stiffening effect when the number of airfoil increases.

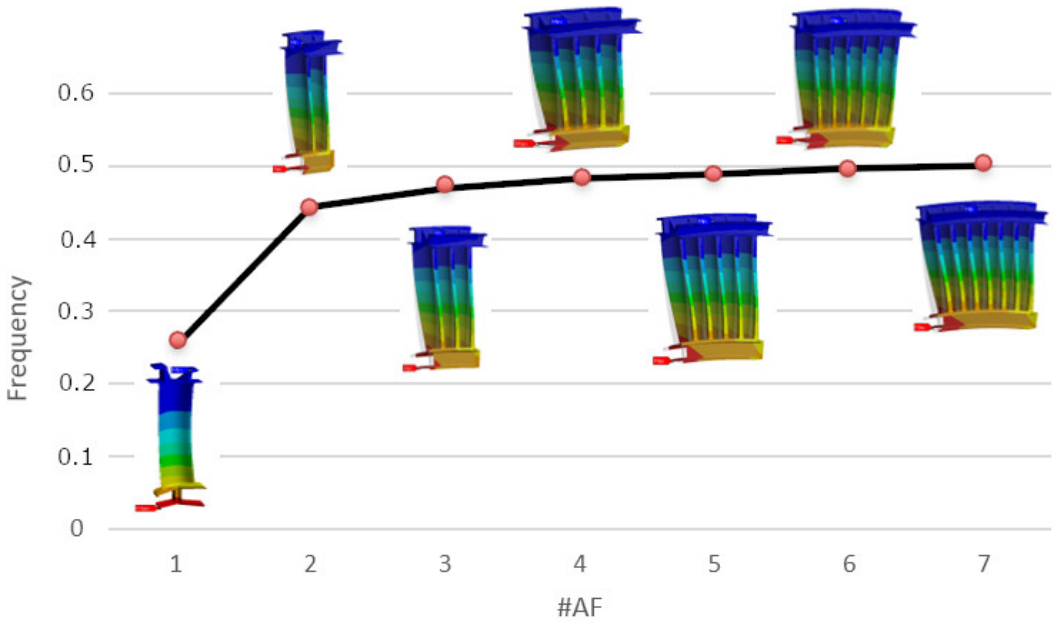

Figure 6.10: Trend of frequency due to the Airfoil Count per Segment effect

Chapter 7

Conclusion and Future Work

This thesis was based on contribution to the development of a tool whose main goal is the improvement of the preliminary design making the project process more robust and smart. In particular, this work focused on the substantial modification of the in house developed tool code (DynBooster) that deals with the CAD generation. As a result, improvements have been obtained on CAD generation times, capabilities extensions, management of multiple templates as well as a flexible operating logic.

Furthermore, the process of creating parametric templates has been completely redefined, based on a simple and robust logic. This has allowed not only to reduce the generation time of a template that could be achieved with just a few steps, but also to create more complex components that better match the reality.

The generation of multiple templates has led to the development of a new graphical interface through which the user can customize the templates. It is important to underline how this progress made it possible to generate around 96 new possible templates configurations, an excellent starting point for the development of innovative LPT configurations.

The introduction of the disk template with the subsequent integration within the DynBoster process has defined a further working mode of the tool. In other words, with this new version of DynBooster, it is possible to generate blade only, vane, blade/disk and many other new configurations.

An important simplification of the CAD creation process is based on external tool (Converter) that automates the process of creating tmpl files (files containing the parameters groups used in defining the template) and determines the conversion from imperial to metric and opposite.

As a last step, the new version od DynBooster has been integrated with wizard (the current process FEM generation build in ANSYS Workbench), and tested with new configuration blades, finding good results and properly validated. Finally, the next short-term goal is to integrate the blade/disk analysis into the wizard with appropriate conditions ad introduce the hollow blades into DynBooster tool. The

long-term goal concerns the introduction of a producibility package. This plug-in will allow to take into account the manufacturing process capability within the CAD model generation by adding dimensioning and tolerancing optimizations.

Appendices

Appendix A

Converter tool

The converter is an external tool developed with the purpose to reach the following goals:

- Generate automatically the structure of tmpl files, taking the prt files as reference. The tmpl files are one of the core files used in templating, has a defined structure and contains the follow parameters groups: system, couple, custom and general information. Whereas the prt files are part file created by Unigraphic NX and including a 3D model and part structure.
- It can extract the file tmpl from prt file and convert the latter from imperial to metric and the opposite.

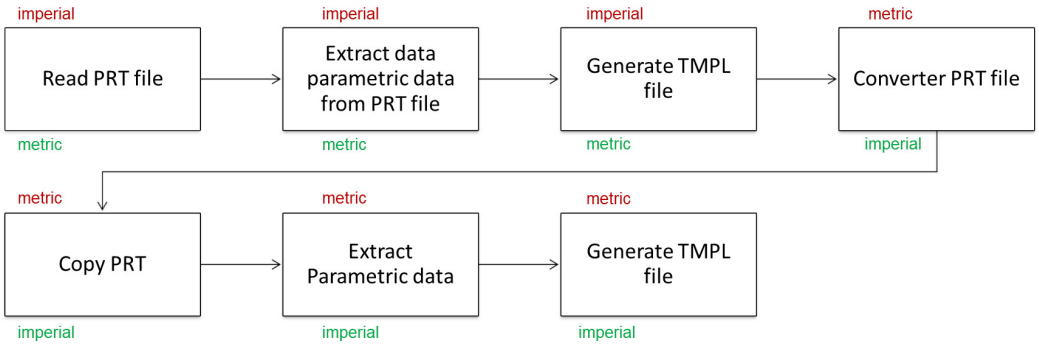

Figure A.1: Converter workflow

The tool has been completely written in Matlab and provides a GUI (graphical user interfaces), where the user can select one or more prt file to converter. Moreover, the reference length must be inserted taking from cross-section, and used to calculate the scale factor.

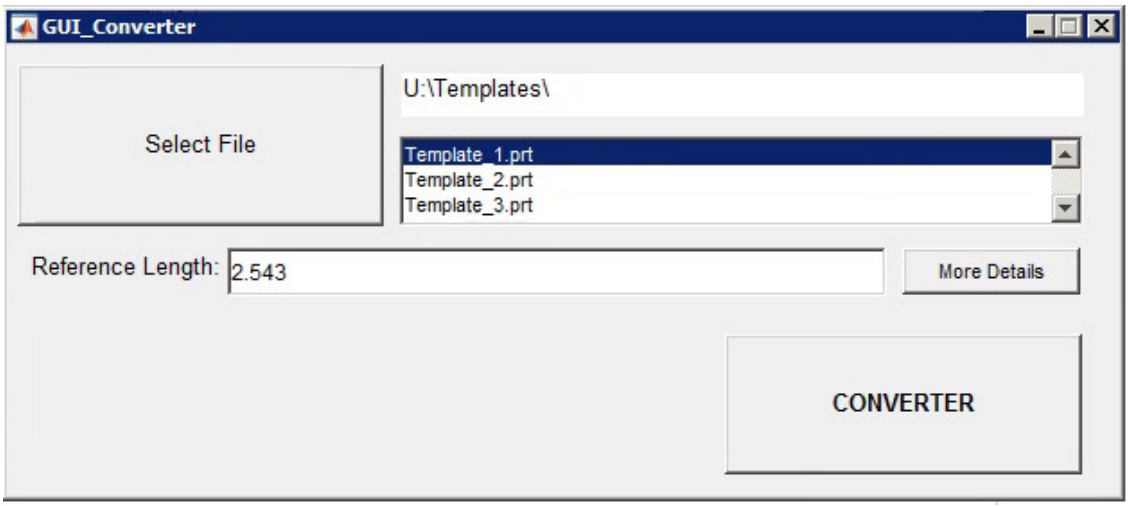

Figure A.2: Converter, Graphical User Interface (GUI)

In particular the code is making it possible to release a visual basic file and run the latter through an executable contained in the NX directory. This procedure allows to perform the extraction and conversion operations.

Appendix B

Validation Procedure between Nastran-Workbench

All the analyses defined in 6.3.1 paragraph, are performed in Ansys Workbench environment, while the Avio Aero legacy is built based on MSC Nastran software. This is the reason such that the validation process between Nastran-Workbench is introduced. Indeed, the following table shows the percentage error between Nastran Workbench solution by means of the formulation:

$$e = \frac{|f_N - f_{WB}|}{f_N} \cdot 100[\%] \tag{B.1}$$

Where f_N is the Nastran frequency, whereas F_WB is the workbench frequency.

Cold e[%]	*Cruise e[%]*	*Take-off e[%]*	*Design poiny e [%]*
0.07	0.24	0.29	0.37
0.03	0.24	0.27	0.33
0.04	0.04	0.047	0.33
0.03	0.03	0.34	0.27
0.07	0.17	0.21	0.16
0.98	1.21	1.44	0.30
0.20	0.22	0.24	0.23
0.05	0.05	0.08	0.03
0.34	0.39	0.42	0.43
0.25	0.24	0.29	0.27

Table B.1: Relative error on frequency base between Nastran-Workbench

From table shown that, the errors fluctuate from values close to zero to values that can even exceed 1%. These results are acceptable as we are considering the comparison between the Nastran solution and Workbench project defined by PRIME. On the other hand, we expect results to be considerably less than 1% when

comparing Nastran and Workbench project. In other words when considering the design practice of the company, the mesh and material are imported from Nastran to Workbench.

Bibliography

[1] Regione Piemonte. *Great 2020*. 2012. URL: \url{http://www.great2020.it/index.html}.

[2] F. Gamma F. Nasuti D. Lentini. *Dispense del Corso di Propulsione Aerospaziale*. Università degli Studi di Roma "La Sapienza, 2004/05.

[3] L. Casalino and D. Pastrone. *Fondamenti di macchine*. Appunti accademici "Politecnico di Torino, 2014.

[4] Luca Cipressa. "Study of new simulation method for lp turbine row, trade-off study and assessment." Tesi di Laurea Magistrale. Politecnico di Torino, 2017.

[5] Rolls-Royce. *The Jet Engine*. Rolls-Royce plc,
fth edition, 1996.

[6] Paolo Turroni. "Studio della dinamica di settori palettati statorici nelle turbomacchine per impiego aeronautico". Tesi di Laurea Magistrale. Politecnico di Torino, 2015.

[7] Fabio Bellacicco. "Stabilizzazione di uno stadio di LPT bladed-disk in presenza della condizione di instabilità a flutter mediante mistuning intenzionale". Tesi di Laurea Magistrale. Politecnico di Torino, 2016.

[8] D. Prino. "Automatic Preliminary Assessment of the mechanical response of LPT stages". Tesi di Laurea Magistrale. Politecnico di Torino, 2018.

[9] Christian Fantino. "Caratterizzazione Dinamica di un Rotore LPT in Presenza di Mistuning Intenzionale". Tesi di Laurea Magistrale. Politecnico di Torino, 2018.

[10] Vito Citera. "Caratterizzazione Dinamica di un Rotore LPT in Presenza di Mistuning Intenzionale". Tesi di Laurea Magistrale. Politecnico di Torino, 2017.

[11] Andrea Bray. "Interazione fluido-struttura in turbine aeronautiche di bassa pressione". Tesi di Laurea Magistrale. Politecnico di Torino, 2017-2018.

[12] Hui Y. *3D Unsteady Flow in Oscillating Compressor Cascade*. Durham theses, Durham University, 2004.

[13] A.V. Srinivasan. *Flutter and Resonant Vibration Characteristics of Engine Blades.* Journal of Engineering for Gas Turbines and Power, Vol.119, 1997.

[14] John J. Vargo Murari P. Singh. *Safe diagram - a design and reliability tool for turbine blading.* Proceedings of the seventeenth turbomachinery symposium, 1988.

[15] Neville F. Rieger. *The Relationship Between Finite Element Analysis and Modal Analysis.* Stress Technology Incorporated, Rochester, New York, 1992.

[16] TM Berruti G Battiato CM Firrone. *Reduced order modeling for multi-stage coupling of cyclic symmetric structures.* In International Conference on Noise and Vibration Engineering, 2016.

[17] P.J. Koch J.P. Clark and S.L. Puterbaugh. *Highly loaded low-pressure turbine: design, numerical and experimental analysis.* Interim Report, University of Notre Dame, 2010.

[18] Giuseppe Battiato. "Vibrations prediction and measurement of multi-stage bladed disks with non linear behavior due to friction contacts." Phd Thesis. Politecnico di Torino, 2017.

[19] Andrea Ferrante. "Sviluppo di un tool per studio dinamico automatizzato relativo a palette di turbine di bassa pressione". Tesi di Laurea Magistrale. Politecnico di Torino, 2018.